Lithos 48 (1999) 237–262

# Erosion of lithospheric mantle beneath the East African Rift system: geochemical evidence from the Kivu volcanic province

Tanya Furman [a,*], David Graham [b]

[a] Department of Geosciences, The Pennsylvania State University, University Park, PA 16802, USA
[b] College of Oceanic and Atmospheric Sciences, Oregon State University, Corvallis, OR 97331, USA

Received 20 April 1998; received in revised form 9 February 1999; accepted 10 February 1999

**Abstract**

This study presents new major and trace element and Sr–Nd isotopic results for a suite of Miocene–Recent mafic lavas from the Kivu volcanic province in the western branch of the East African Rift. These lavas exhibit a very wide range in chemical and isotopic characteristics, due to a lithospheric mantle source region that is heterogeneous on a small scale, probably $< 1$ km. The chemical and isotopic variations are mostly geographically controlled: lavas from Tshibinda volcano, which lies on a rift border fault on the northwestern margin of the province, have higher values of $^{87}Sr/^{86}Sr$, $(La/Sm)_n$, Ba/Nb, and Zr/Hf than the majority of Kivu (Bukavu) samples. The range of $^{87}Sr/^{86}Sr$ at Tshibinda (0.70511–0.70514) overlaps some compositions found in the neighboring Virunga province, while Bukavu group lavas include the lowest $^{87}Sr/^{86}Sr$ (0.70314) and highest $\varepsilon_{Nd}$ (+7.6) yet measured in western rift lavas. The Tshibinda compositions trend towards a convergence for Sr–Nd–Pb isotopic values among western rift lavas. Among Kivu lavas, variations in $^{143}Nd/^{144}Nd$ correlate with those for certain incompatible trace element ratios (e.g., Th/Nb, Zr/Hf, La/Nb, Ba/Rb), with Tshibinda samples defining one compositional extreme. There are covariations of isotopic and trace element ratios in mafic lavas of the East African Rift system that vary systematically with geographic location. The lavas represent a magmatic sampling of variations in the underlying continental lithospheric mantle, and it appears that a common lithospheric mantle (CLM) source is present beneath much of the East African Rift system. This source contains minor amphibole and phlogopite, probably due to widespread metasomatic events between 500 and 1000 Ma. Lava suites which do not show a strong component of the CLM source, and for which the chemical constraints also suggest the shallowest magma formation depths, are the Bukavu group lavas from Kivu and basanites from Huri Hills, Kenya. The inferred extent of lithospheric erosion therefore appears to be significant only beneath these two areas, which is generally consistent with lithospheric thickness variations estimated from gravity and seismic studies. 

*Keywords:* East African Rift system; Kivu volcanic province; Lithospheric mantle; Basalt geochemistry; Continental rifting

## 1. Introduction

The subcontinental lithospheric mantle (SCLM) comprises the basal part of the Earth's outer rigid mechanical boundary layer, and may also represent a chemical and/or thermal boundary layer in the shallowest mantle (Harry and Leeman, 1995). The SCLM can contain old portions of mantle with distinctive trace element and isotope characteristics, due to prolonged isolation from underlying asthenospheric convection (McDonough, 1990). It is thought to have originated and evolved as a residue of ancient partial

* Corresponding author


PII: S0024-4937(99)00031-6

melting followed by the polybaric crystallization of silicate melts and hydrous fluids (Hawkesworth et al., 1990). Direct evidence on its composition comes from mantle xenoliths entrained in continental lavas. The small size and limited spatial distribution of xenoliths, however, may not provide an accurate representation of regional variations in the composition of the SCLM. Continental volcanic rocks, particularly silica-undersaturated mafic lavas, may be especially useful for this purpose. Such lavas are often taken to represent partial melts of the SCLM, formed either above a thermal anomaly such as a mantle plume, or during tectonic extension and associated continental rifting.

In this study, we investigate the geochemistry of Miocene to Recent mafic lavas from the Kivu volcanic province, located in the western branch of the East African Rift, in order to document changes in melt composition associated with lithospheric thinning above a hypothesized mantle plume. We interpret the extreme heterogeneity in isotopic and incompatible trace element abundance ratios found in Kivu lavas to be indicative of dramatic changes in mantle source composition following the onset of volcanism near 12 Ma. By comparing the trace element and isotopic results from Kivu with earlier studies from throughout the eastern and western rift branches, we find evidence for a common lithospheric mantle (CLM) source that has been sampled by lavas over an area of approximately $10^6$ km$^2$. The mineralogy of this common source includes minor amphibole and phlogopite, and may be similar in composition to the oceanic lithospheric mantle described by Class and Goldstein (1997). In the East African Rift system, variations in the inferred relative abundances of hydrous phases (amphibole and phlogopite) in the mantle source are also related to Sr and Nd isotopic differences, consistent with a multistage metasomatic history for the continental lithospheric mantle in this region.

## 2. Background

### 2.1. Geodynamic setting of the East African Rift system

The East African Rift system (Fig. 1) traverses two regions of topographic uplift, the Ethiopian and Kenyan domes, separated by a zone of NW–SE trending extension (Anza graben). A second NW–SE trending rift that includes Lakes Tanganyika, Rukwa and Malawi defines the southern extent of the Kenyan dome. Between these borders, the rift system comprises two branches, separated by the ~1300 km-wide East African plateau.

The Kenyan dome is believed to overlie an upwelling plume head that has begun to flatten beneath the continental lithosphere (White and McKenzie, 1989; Griffiths and Campbell, 1991). Detailed geophysical work both along the rift axes and across the East African plateau has helped reveal some of the dynamics of plume encroachment. Recent profiles (summarized in Simiyu and Keller, 1997) indicate a broad ($1200 \pm 100$ km wide) negative gravity anomaly associated with the Kenya dome that extends westward to Lakes Edward and Kivu and southeastward into Tanzania. The regional gravity study of Ebinger et al. (1989) found that topographic wavelengths $> 1000$ km are overcompensated across the Kenyan dome, suggesting that surface features are maintained by dynamic uplift from the upper mantle. Taken together, these observations suggest that a hot mantle plume is centered beneath the northern part of the Tanzanian craton and Lake Victoria, and model calculations are consistent with a plume head diameter of 600 km (Simiyu and Keller, 1997).

Superposed on the gravity signature of the plateau are narrow, steep-sided negative anomalies that define the boundary between Proterozoic orogenic belts and the Archean Tanzanian craton and that are coincident with the rift valleys themselves (Simiyu and Keller, 1997). Detailed gravity studies (Upcott et al., 1996; Simiyu and Keller, 1997) suggest that the underlying mantle plume has two arms with diameters $< 250$ km that penetrate the lithosphere to shallow levels beneath the eastern and western rift branches. The gravity anomaly associated with the eastern rift is shallowest beneath north central Kenya and deepens rapidly to the north and south (Simiyu and Keller, 1997). In the western rift, the geophysical data suggest that the greatest extent of lithospheric thinning has occurred just south of the Kivu volcanic province. Experimental investigations of plume dynamics (Griffiths and Campbell, 1991) also suggest that the narrow, arcuate western rift may

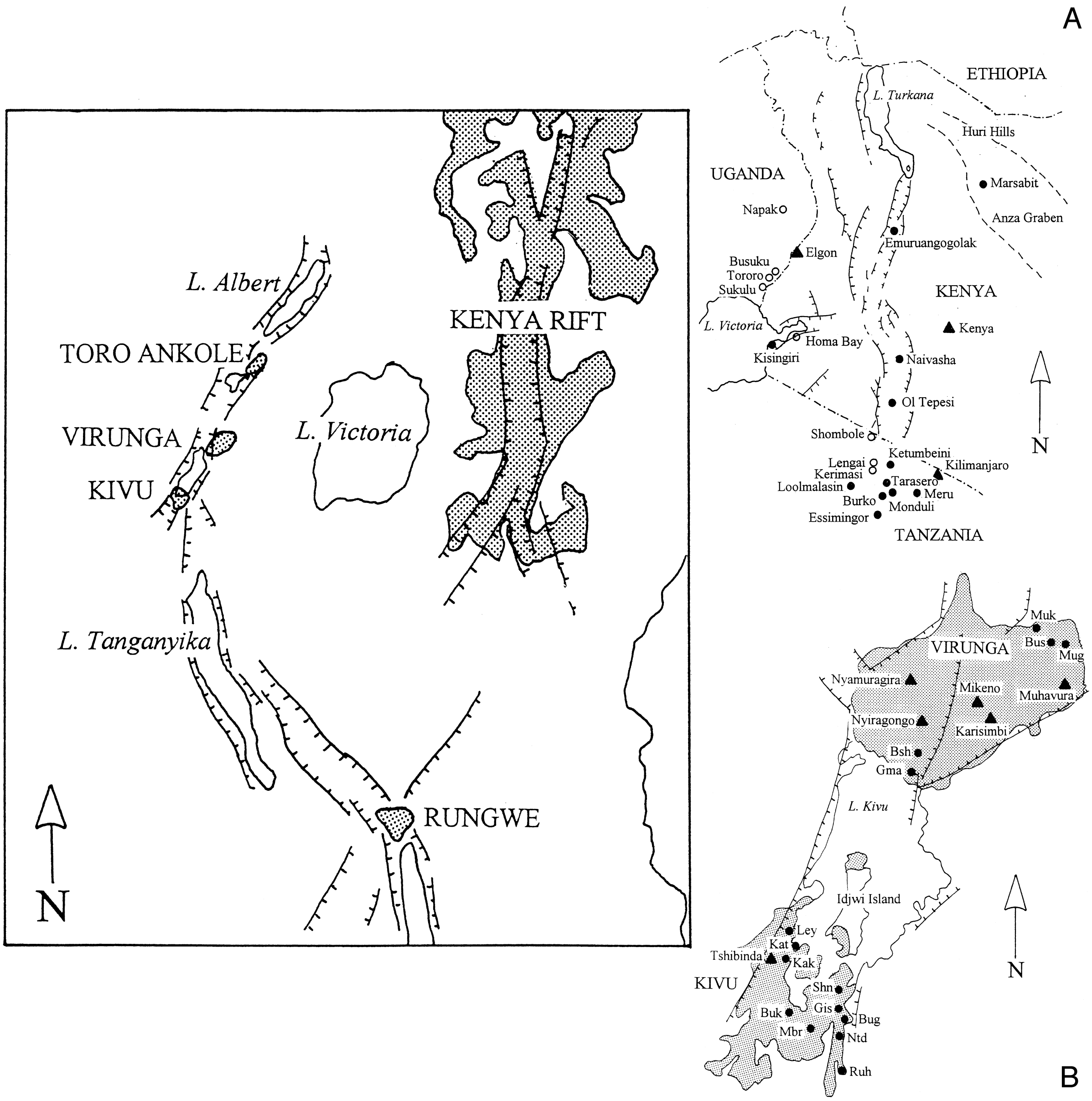


Fig. 1. Map of the East African Rift system. Insets show locations discussed in the text. Areas of Miocene to Recent volcanism are shaded. Inset (A): eastern branch. Centers of mafic silicate volcanism mentioned in the text are indicated by filled circles, carbonatite localities are indicated by open circles. Filled triangles are major off-rift volcanic edifices. Inset (B): sketch maps of the Kivu and Virunga volcanic provinces, with areas of post-Miocene volcanism shaded. Volcanic centers are indicated by filled triangles, and smaller vents by filled circles. Key to Kivu sample localities: Bug — N. Bugarama; Buk — Bukavu; Gis — Gisakura; Kak — Kakondo; Kat — Katana; Ley — Leymera; Mbr — Mbirizi; Ntd — Ntode River; Ruh — Ruhagarika; Shn — Shangazi River. Key to Virunga vents: Gma — Goma; Bsh — Bushwaga; Muk — Mukuvu; Bus — Busamba; Mug — Muganza.

reflect subsidence of cold lithospheric mantle near the edge of a plume head. This model is consistent with the low degree of extension estimated for the western rift ( < 15%; Ebinger, 1989b), and may be appropriate for parts of the eastern rift as well. Under this scenario, the post-Miocene alkalic volcanism throughout the East African Rift system is primarily caused by melting of lithospheric mantle.

Table 1
Major and trace element analyses of Kivu lavas
Sample prefixes: B = Burundi, R = Rwanda, Z = Zaire (Congo).
Major and selected trace elements (Rb, Sr, Ba, Zn, Ni, V, Y, Nb, Zr, La, Ce) were determined by X-ray fluorescence (XRF) on fused disks (major elements) and pressed powder pellets (trace elements) at the University of Massachusetts (Amherst). Instrumental neutron activation analyses for the REE, Co, Cr, Hf, Sc, Ta, Th were performed on splits of the same samples at the Massachusetts Institute of Technology. Where only La and Ce are reported, these values were analyzed by XRF; when all REE are reported, the INAA values are used for La and Ce. One-sigma precision estimates for XRF and INAA based on replicate analyses are: major elements (except MnO) < 1%; La, Cr, Co, Hf, Sc, Ba, Rb, y, Sr, Ni, V, Zn, Zr < 2%; remaining REE, Nb, Ta, MnO 2–5%; Tb, Th 5–10%.

| Sample | Unit | Location | $SiO_2$ | $TiO_2$ | $Al_2O_3$ | $Fe_2O_3$ | MnO | MgO | CaO | $Na_2O$ | $K_2O$ |
|---|---|---|---|---|---|---|---|---|---|---|---|
| B10C | Tv2 | Ruhagarika | 50.00 | 1.90 | 14.16 | 11.89 | 0.19 | 6.70 | 11.50 | 2.74 | 0.49 |
| R3L | Tv1 | Bugarama | 44.89 | 2.91 | 14.26 | 12.88 | 0.21 | 8.93 | 10.17 | 3.44 | 1.35 |
| R5N | Qv | Gisakura | 45.85 | 2.54 | 14.58 | 12.08 | 0.25 | 9.09 | 10.21 | 3.43 | 1.23 |
| R2J | Tv2 | Mbirizi | 48.24 | 2.33 | 15.51 | 10.31 | 0.17 | 8.07 | 9.36 | 3.25 | 1.89 |
| R6C | Tv2 | Mbirizi | 44.63 | 2.20 | 14.62 | 11.43 | 0.22 | 10.07 | 11.53 | 3.14 | 1.15 |
| R4HA | Tv | Mbirizi | 45.31 | 2.26 | 13.28 | 11.88 | 0.20 | 11.37 | 11.70 | 2.28 | 1.04 |
| R3K | Tv1 | Ntode R. | 51.42 | 2.16 | 16.61 | 12.56 | 0.13 | 4.90 | 6.77 | 3.17 | 1.51 |
| R4Q | Tv | Shangazi R. | 45.27 | 2.26 | 12.95 | 11.82 | 0.20 | 11.94 | 11.52 | 2.74 | 0.52 |
| R5A1 | Tv | Shangazi R. | 45.79 | 2.21 | 13.44 | 11.86 | 0.20 | 10.95 | 11.30 | 2.68 | 1.05 |
| R5A3 | Tv | Shangazi R. | 45.35 | 2.24 | 13.33 | 11.75 | 0.20 | 11.24 | 11.32 | 2.96 | 1.11 |
| Z6G | Tv | Kakondo | 46.99 | 1.54 | 14.96 | 12.60 | 0.20 | 9.28 | 10.76 | 2.48 | 0.80 |
| Z4H1 | Tv | Katana | 49.35 | 1.43 | 16.05 | 10.93 | 0.16 | 7.19 | 10.02 | 3.29 | 0.83 |
| Z7Z | Qv | Leymera | 46.60 | 1.93 | 15.55 | 11.85 | 0.23 | 8.69 | 10.55 | 3.17 | 1.03 |
| Z6A | Tv1 | NW Bukavu | 46.56 | 1.99 | 14.63 | 10.78 | 0.20 | 8.27 | 11.20 | 3.77 | 1.42 |
| Z6B | Tv1 | NW Bukavu | 46.74 | 1.99 | 14.61 | 10.85 | 0.20 | 8.72 | 10.92 | 3.52 | 1.39 |
| Z3C1 | Qv | Tshibinda | 46.63 | 1.49 | 14.18 | 11.41 | 0.19 | 9.10 | 11.92 | 3.21 | 1.03 |
| Z3C2 | Qv | Tshibinda | 46.21 | 1.49 | 14.05 | 11.32 | 0.20 | 8.83 | 12.15 | 2.99 | 1.57 |
| Z3D | Qv | Tshibinda | 46.10 | 1.50 | 14.02 | 11.05 | 0.19 | 8.74 | 12.11 | 3.61 | 1.55 |
| Z5G | Qv | Tshibinda | 46.49 | 1.53 | 14.35 | 11.27 | 0.20 | 8.76 | 12.47 | 2.99 | 0.94 |

| Sample | Unit | Location | Rb | Cs | Sr | Ba | Sc | V | Cr | Co | Ni | Zn |
|---|---|---|---|---|---|---|---|---|---|---|---|---|
| B10C | Tv2 | Ruhagarika | 15 | 0.14 | 353 | 230 | 24.0 | 173 | 245 | 46.3 | 147 | 115 |
| R3L | Tv1 | Bugarama | 36 | 0.38 | 727 | 577 | 23.4 | 212 | 221 | 52.1 | 143 | 110 |
| R5N | Qv | Gisakura | 34 | – | 688 | 654 | – | 218 | 255 | – | 182 | 101 |
| R2J | Tv2 | Mbirizi | 46 | 0.39 | 768 | 701 | 21.0 | 192 | 216 | 46.8 | 144 | 94.9 |
| R6C | Tv2 | Mbirizi | 35 | – | 667 | – | – | – | – | – | – | – |
| R4HA | Tv | Mbirizi | 30 | – | 652 | – | – | – | – | – | – | – |
| R3K | Tv1 | Ntode R. | 33 | – | 401 | 767 | – | 135 | 237 | | 187 | 124 |
| R4Q | Tv | Shangazi R. | 28 | 0.47 | 585 | 536 | 30.1 | 241 | 442 | 58.7 | 268 | 99.4 |
| R5A1 | Tv | Shangazi R. | 27 | – | 768 | – | – | – | – | – | – | – |
| R5A3 | Tv | Shangazi R. | 31 | 0.2 | 587 | 611 | 29.8 | 228 | 411 | 63.3 | 248 | 98.5 |
| Z6G | Tv | Kakondo | 23 | – | 460 | 536 | – | 230 | 355 | – | 218 | 103 |
| Z4H1 | Tv | Katana | 16 | bdl | 623 | 783 | 23.2 | 175 | 206 | 46.5 | 115 | 91.0 |
| Z7Z | Qv | Leymera | 31 | 0.14 | 710 | 718 | 26.8 | 207 | 267 | 60.5 | 146 | 88.0 |
| Z6A | Tv1 | NW Bukavu | 36 | 0.3 | 1247 | 1014 | 22.0 | 189 | 304 | 45.5 | 162 | 89.9 |
| Z6B | Tv1 | NW Bukavu | 35 | 0.35 | 1198 | 977 | 22.6 | 188 | 304 | 53.3 | 171 | 91.6 |
| Z3C1 | Qv | Tshibinda | 55 | – | 737 | 768 | – | 208 | 315 | – | 187 | 94.0 |
| Z3C2 | Qv | Tshibinda | 47 | 0.66 | 821 | 1175 | 28.4 | 193 | 309 | 55.7 | 171 | 91.6 |
| Z3D | Qv | Tshibinda | 52 | 0.51 | 867 | 1310 | 28.4 | 203 | 305 | 53.8 | 151 | 85.4 |
| Z5G | Qv | Tshibinda | 66 | – | 898 | 1235 | – | 186 | 284 | – | 172 | 102 |

Volcanism and uplift began roughly contemporaneously in the eastern rift ca. 23 Ma, and in the western rift ca. 12 Ma (Bellon and Pouclet, 1980; Kampunzu et al., 1986; Ebinger, 1989a; Pasteels et

| $P_2O_5$ | Total | Mg# |
|---|---|---|
| 0.29 | 99.86 | 56.75 |
| 0.94 | 99.99 | 61.77 |
| 0.62 | 99.88 | 63.66 |
| 0.63 | 99.76 | 64.54 |
| 0.76 | 99.75 | 67.19 |
| 0.56 | 99.88 | 69.02 |
| 0.50 | 99.73 | 47.60 |
| 0.55 | 99.76 | 70.15 |
| 0.51 | 99.98 | 68.27 |
| 0.54 | 100.04 | 69.04 |
| 0.37 | 99.98 | 63.19 |
| 0.49 | 99.74 | 60.48 |
| 0.65 | 100.25 | 63.15 |
| 0.90 | 99.72 | 64.09 |
| 0.90 | 99.83 | 65.17 |
| 0.66 | 99.81 | 65.00 |
| 0.79 | 99.59 | 64.42 |
| 0.78 | 99.65 | 64.77 |
| 0.82 | 99.82 | 64.40 |

| Y | Zr | Nb | Hf | Ta | Th | U | Pb | La | Ce | Nd | Sm | Eu | Tb | Yb | Lu |
|---|---|---|---|---|---|---|---|---|---|---|---|---|---|---|---|
| 26 | 132 | 29.1 | 3.0 | 1.1 | 4.1 | 2 | 3 | 24.8 | 49.7 | 20.0 | 4.69 | 1.57 | 0.81 | 2.16 | 0.30 |
| 35 | 290 | 65.4 | 5.8 | 3.2 | 4.2 | 2 | 4 | 44.8 | 93.0 | 44.9 | 9.72 | 3.15 | 1.31 | 2.69 | 0.40 |
| 31 | 247 | 70.3 | – | – | 7.0 | 3 | 5 | 52.1 | 93.7 | – | – | – | – | – | – |
| 29 | 283 | 79.4 | 5.9 | 3.8 | 5.5 | 2 | 4 | 45.2 | 91.7 | 38.9 | 8.03 | 2.50 | 1.00 | 2.53 | 0.33 |
| 31 | – | – | – | – | 7.0 | 3 | 5 | – | – | – | – | – | – | – | – |
| 28 | – | – | – | – | 6.0 | 2 | 3 | – | – | – | – | – | – | – | – |
| 76 | 219 | 58.3 | | | 6.0 | 2 | 4 | 117 | 99.0 | | | | | | |
| 28 | 191 | 72.1 | 4.0 | 3.3 | 6.8 | 2 | 3 | 49.0 | 95.6 | 40.1 | 7.88 | 2.37 | 1.01 | 2.43 | 0.33 |
| 27 | – | – | – | – | 6.0 | 2 | 5 | – | – | – | – | – | – | – | – |
| 29 | 203 | 70.1 | 4.1 | 3.3 | 7.0 | 3 | 5 | 49.2 | 98.0 | 40.6 | 7.82 | 2.35 | 1.03 | 2.41 | 0.33 |
| 31 | 122 | 56.0 | – | – | 6.0 | 1 | 5 | 41.3 | 68.8 | – | – | – | – | – | – |
| 25 | 127 | 63.7 | 2.5 | 2.5 | 10.2 | 3 | 6 | 59.9 | 102 | 32.8 | 5.44 | 1.74 | 0.83 | 2.10 | 0.32 |
| 29 | 207 | 95.2 | 4.4 | 4.3 | 7.7 | 2 | 4 | 60.4 | 114 | 39.0 | 6.91 | 2.21 | 0.92 | 2.87 | 0.40 |
| 29 | 241 | 124 | 4.3 | 5.5 | 11.3 | 6 | 5 | 94.7 | 179 | 63.9 | 10.2 | 2.88 | 1.08 | 2.35 | 0.30 |
| 30 | 235 | 122 | 4.3 | 5.0 | 10.4 | 6 | 6 | 93.2 | 173 | 61.5 | 10.0 | 2.95 | 1.09 | 2.37 | 0.36 |
| 27 | 144 | 87.3 | – | – | 12.0 | 3 | 5 | 70.0 | 117 | – | – | – | – | – | – |
| 27 | 155 | 99.6 | 3.1 | 4.3 | 13.8 | 4 | 6 | 76.7 | 133 | 47.0 | 7.79 | 2.20 | 0.95 | 2.48 | 0.39 |
| 27 | 143 | 98.6 | 3.3 | 4.2 | 12.8 | 4 | 7 | 77.3 | 132 | 44.3 | 7.61 | 2.22 | 0.95 | 2.75 | 0.37 |
| 28 | 160 | 103 | – | – | 14.0 | 3 | 5 | 86.7 | 138 | – | – | – | – | – | – |

al., 1989). Mid-Miocene to Recent volcanic activity has occurred along the entire length of the eastern rift, but is restricted to four intrabasinal accommodation zones in the western rift (Ebinger, 1989a,b; Fig. 1). The diversity of mafic volcanic rocks erupted along the eastern and western branches of the rift system has been well-documented (e.g., Holmes and Harwood, 1937; Holmes, 1940, 1950; Bell and Powell, 1969; Bell and Doyle, 1971; Mitchell and Bell, 1976; Baker et al., 1977; De Mulder et al., 1986; Auchapt et al., 1987; Davies and Lloyd, 1989; Marcelot et al., 1989; Lloyd et al., 1991; Rogers et al., 1992, 1998; Class et al., 1994; Furman and Graham, 1994; Furman, 1995; Paslick et al., 1995), and can be used to investigate the interaction between magmas derived from asthenospheric and lithospheric sources beneath this region of the African plate.

### 2.2. The Kivu volcanic province

The Kivu volcanic province is located in the western branch of the East African Rift, along the borders of Rwanda, Burundi and eastern Zaire (Congo). It includes two discrete volcanic fields: Bukavu, which covers an area roughly $35 \times 35$ km$^2$ near Lake Kivu, and Mwenga-Kamituga, located 80 km to the southwest. Samples from this study come from Bukavu and include four lavas from Tshibinda volcano (Fig. 1). The Kivu area comprises three sedimentary basins defined by border faults, and its volcanism is intimately linked to faulting during basin formation (Ebinger, 1989a).

Three cycles of volcanic activity have been recognized at Bukavu (Kampunzu et al., 1986; Ebinger, 1989a; Pasteels et al., 1989), each of which is dominated by fissure eruptions of mafic lavas. Earliest activity (unit Tv1) occurred prior to rifting, between roughly 10 and 7.5 Ma and is limited to the East Kivu basin and the southern part of Idjwi Island. Mafic lavas from this period include olivine- and quartz-normative tholeiites. Second-stage volcanism (unit Tv2), which likely corresponds to the start of rift formation, occurred between $\sim 7.5$ and 4 Ma in both the East and West Kivu basins. Lavas erupted along the rift boundary faults during this episode include sodic alkali basalts and basanites in addition to minor volumes of trachytes and phonolites. The third stage of volcanic activity (Qv) includes tholeiitic and alkalic basalts erupted primarily along the West Kivu border fault system. Tshibinda volcano is one of the most recently active volcanic centers located on this fault. The West Kivu border fault has served as the master fault for crustal extension during the Quaternary, and forms a structural link between the Kivu and Virunga provinces (Ebinger, 1989a).

Samples for this study are mafic lavas from each eruptive cycle (Table 1). Samples from Tshibinda

Table 2
Sr and Nd isotope results for Kivu volcanic province lavas
th = tholeiite, ab = alkali basalt.
Sr and Nd isotope analyses were performed at the University of California (Santa Barbara) on a Finnegan MAT 261 multicollector mass spectrometer, operated in static mode for Sr and in dynamic mode for Nd. Sr was normalized within-run to $^{86}Sr/^{88}Sr = 0.1194$, and adjusted to a value of 0.710250 for NBS 987 (the mean value measured during the course of the study was 0.710199). Nd was normalized within-run to $^{146}Nd/^{144}Nd = 0.721900$. The mean value measured for the Ames Nd standard during the course of the study was 0.511890. In addition, $^{143}Nd/^{144}Nd$ ratios measured for two separate dissolutions of BCR-1 were 0.512640 and 0.512629. Chemical separations followed procedures outlined in (Hoernle, 1990). Briefly, approximately 100 mg of whole rock powder was leached in 2 N HCl for 1 h at 50°C, then rinsed several times with ultrapure distilled water; prior to overnight dissolution in $HF + HClO_4$, Sr and Nd were sequentially separated by a series of ion-exchange chromatography columns. Blanks for Sr and Nd were $\sim 0.3$ and $< 1$ ng, respectively, which is insignificant for the samples studied here.

| Location | Sample | Type | $^{87/86}Sr$ | ± | $^{143/144}Nd$ | ± | $\varepsilon_{Nd}$ |
|---|---|---|---|---|---|---|---|
| Ruhagarika | B10C | th | 0.704409 | 8 | 0.512838 | 6 | 3.90 |
| N Bugarama | R3L | ab | 0.703138 | 9 | 0.513026 | 7 | 7.57 |
| Gisakura | R5N | ab | 0.703493 | 8 | 0.512925 | 7 | 5.60 |
| Mbirizi | R2J | ab | 0.703816 | 9 | 0.512907 | 5 | 5.25 |
| Mbirizi | R6C | ab | 0.703575 | 10 | 0.512888 | 6 | 4.88 |
| Mbirizi | R4HA | ab | 0.703999 | 12 | 0.512870 | 5 | 4.53 |
| Ntode R. | R3K | ab | 0.704931 | 11 | 0.512749 | 5 | 2.17 |
| Shangazi R. | R4Q | ab | 0.703930 | 9 | 0.512871 | 6 | 4.55 |
| Shangazi R. | R5A1 | ab | 0.704234 | 12 | 0.512841 | 8 | 3.96 |
| Shangazi R. | R5A3 | ab | 0.704037 | 9 | 0.512851 | 7 | 4.15 |
| Kakondo | Z6G | ab | 0.704567 | 8 | 0.512777 | 8 | 2.71 |
| Katana | Z4H1 | th | 0.704365 | 9 | 0.512751 | 7 | 2.20 |
| NW Bukavu | Z6A | ab | 0.703994 | 11 | 0.512815 | 6 | 3.45 |
| NW Bukavu | Z6B | ab | 0.703987 | 10 | 0.512775 | 6 | 2.67 |
| Leymera | Z7Z | ab | 0.703429 | 12 | 0.512899 | 10 | 5.09 |
| Tshibinda | Z3C1 | ab | 0.705106 | 11 | 0.512669 | 7 | 0.60 |
| Tshibinda | Z3C2 | ab | 0.705165 | 10 | 0.512671 | 5 | 0.64 |
| Tshibinda | Z3D | ab | 0.705108 | 12 | 0.512659 | 6 | 0.41 |
| Tshibinda | Z5G | ab | 0.705138 | 11 | 0.512660 | 8 | 0.43 |

volcano and Idjwi Island (Marcelot et al., 1989) are considered together as the ''Tshibinda group'', while remaining lavas are termed the ''Bukavu group''. All lavas contain phenocrysts of olivine and clinopyroxene, with plagioclase feldspar phenocrysts restricted to evolved mafic lavas (Appendix A). The samples were collected by C.J. Ebinger (Leeds, UK) and were analyzed for major and trace elements (Table 1) as well as Sr and Nd isotope ratios (Table 2).

### 2.3. Results

#### 2.3.1. Major and compatible trace elements

The major element variations of Kivu lavas indicate that this lava series cannot be related through fractional crystallization from a common parent. This is supported by the observation that most major element oxides (e.g., $P_2O_5$, Fig. 2; also $TiO_2$, $K_2O$, $Na_2O$ not shown) do not define coherent trends against MgO. Furthermore, $CaO/Al_2O_3$ values for lavas with 7–12 wt.% MgO range from 0.62 to 0.89, but values of ~0.8 are found at all MgO contents within this range (Fig. 2). Four alkali basalts from Tshibinda volcano have nearly uniform compositions (~9 wt.% MgO). Abundances of compatible trace elements indicate that most lavas in this series have fractionated olivine and/or clinopyroxene. The Ni, Cr and Sc contents of lavas with 11–13 wt.% MgO are close to values typical of mantle-derived basalts (Table 1). Abundances of Ni (Fig. 2), Cr and V decrease with decreasing MgO content, while Sc shows no regular variation with MgO or $CaO/Al_2O_3$.

#### 2.3.2. Incompatible trace elements

Incompatible trace element abundances in Kivu lavas (e.g., La; Fig. 2) are not correlated with MgO

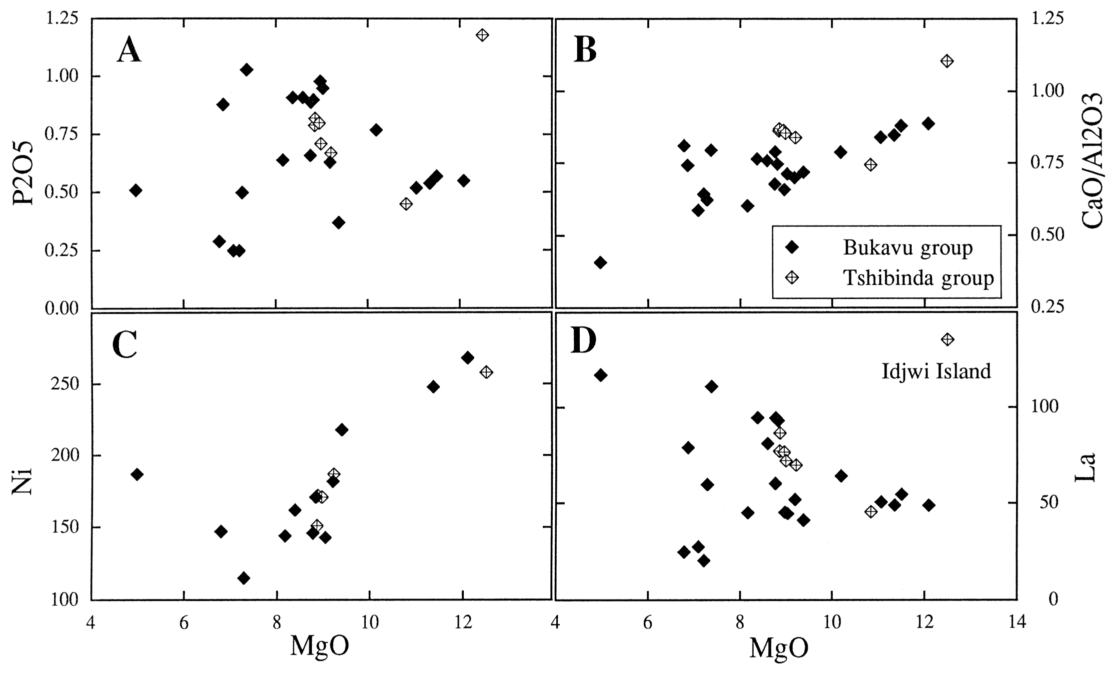


Fig. 2. Variations in major and trace elements among Kivu mafic lavas. Filled diamonds are samples from Rwanda and Burundi (Bukavu group), and crossed diamonds are samples from Tshibinda volcano and Idjwi Island (Tshibinda group). Data are from this study and from Marcelot et al. (1989). (A) Abundances of $P_2O_5$ show no consistent trend with decreasing MgO, indicating the lavas cannot be derived by closed-system fractionation of a single parental mafic magma. (B) Values of $CaO/Al_2O_3$ show little variation among samples with 7–12 wt.% MgO. (C) Abundances of compatible elements such as Ni decrease with decreasing MgO content of Kivu mafic lavas, indicating progressive removal of olivine and/or clinopyroxene. (D) Abundances of incompatible elements such as La increase broadly with decreasing MgO, but the high degree of scatter precludes simple differentiation processes. The primitive alkali basalt from Idjwi Island (sample LKA-4 of Marcelot et al., 1989) has unusually high abundances of most incompatible trace elements.

content. This observation was also made by Marcelot et al. (1989) based on a smaller dataset. The abundances of several incompatible trace elements do correlate strongly with one another. Values of Sr/Ce (Fig. 3) and P/Ce are uniform and fall within the range expected for mantle-derived basalts [mean P/Ce value $56.7 \pm 5.9$, with two outliers, RW88 (Marcelot et al., 1989) and R3L, both from Bugarama and possibly from the same unit, between 102 and 104]. Large ion lithophile elements (LILE; Ba, Rb, Sr) are correlated with one another but not with Th or the high field strength elements (HFSE). Variations between Th, Nb and Zr are geographically controlled (Fig. 3): lavas from the Tshibinda group have higher Th/Nb and Nb/Zr than lavas from the Bukavu group. A similar pattern is found for Ba/La and Ba/Nb, both of which are elevated among Tshibinda group samples.

Chondrite-normalized rare earth element (REE) patterns of Kivu mafic lavas are not parallel (Fig. 4). Highly variable MREE contents lead to crossing patterns that require derivation of the lavas from heterogeneous (or different) mantle sources. Values of $(La/Sm)_n$ are not correlated with La abundances, whereas $(La/Yb)_n$ values are positively correlated with La content (Fig. 5). Lavas from the Tshibinda group have higher $(La/Sm)_n$ than lavas from the Bukavu group (Fig. 5), but crossing REE patterns occur within the latter group as well.

*2.3.3. Sr–Nd isotopes*

Values of $^{87}Sr/^{86}Sr$ and $^{143}Nd/^{144}Nd$ show a strong negative correlation among Kivu lavas (Fig. 6). The range of isotopic ratios is unusually large for such a small area, and requires short-range isotopic

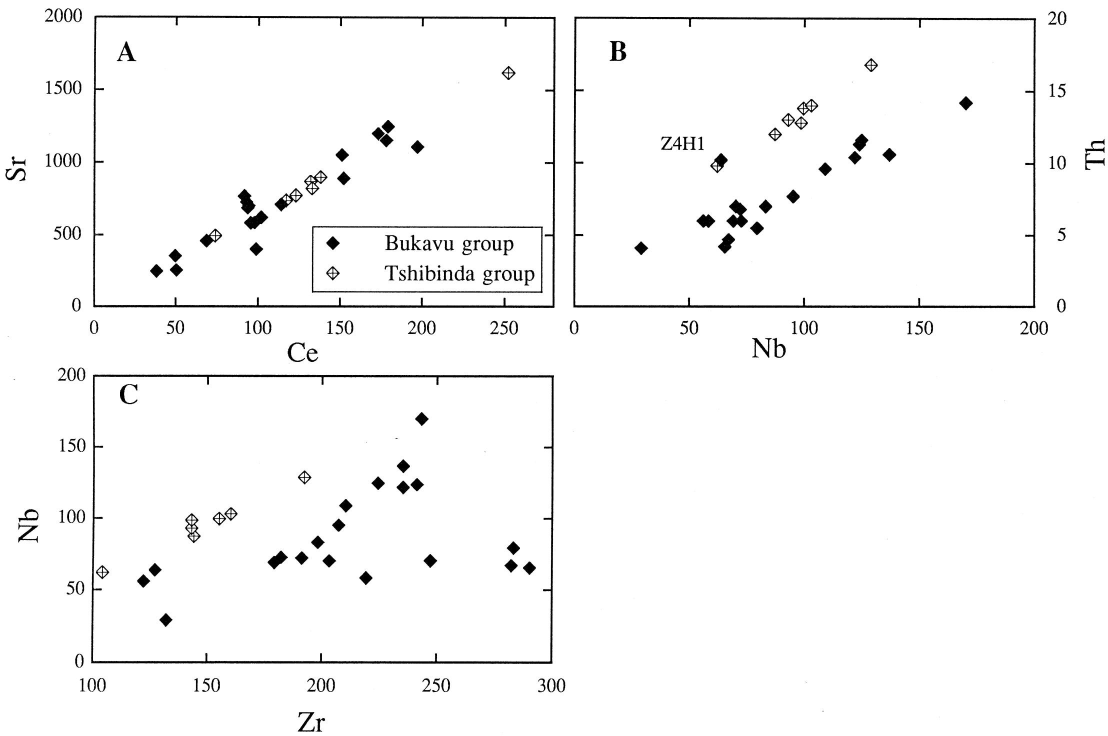


Fig. 3. Incompatible element–element diagrams for Kivu mafic lavas. (A) Sr vs. Ce. Sr and Ce are positively correlated among all Kivu samples with an average Sr/Ce ratios of 6.5, within the range for ocean island basalts but higher than primitive mantle estimates (12; Sun and McDonough, 1989). (B) Th vs. Nb. Th and Nb are positively correlated among Kivu lavas, but samples from the Tshibinda group have higher Th/Nb values (0.14) than samples from the Bukavu group (0.09). The estimated primitive mantle Th/Nb ratio is 0.12 (Sun and McDonough, 1989). (C) Nb vs. Zr. Relative abundances of Nb and Zr show wide variation within the Kivu province, but samples from the Tshibinda group have generally higher Nb at given Zr values than lavas from the Bukavu group.

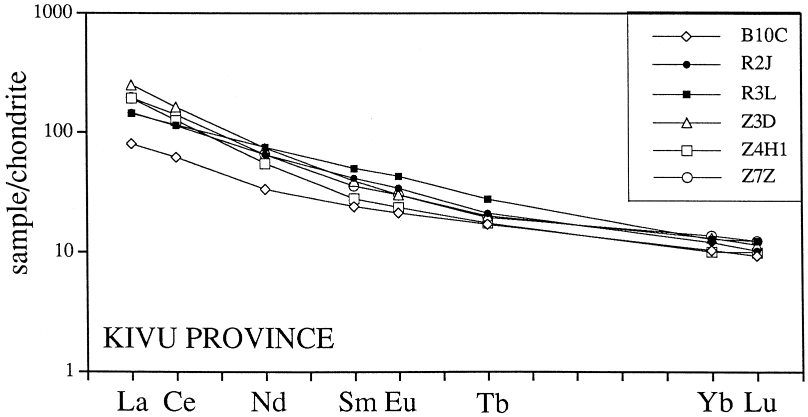


Fig. 4. Chondrite-normalized REE patterns for Kivu mafic lavas. The REE patterns are not parallel, and show large variations in MREE abundances.

heterogeneity in the mantle beneath this region. Four Quaternary lavas from Tshibinda volcano have the highest $^{87}Sr/^{86}Sr$ values (0.70511–0.70514) and lowest $\varepsilon_{Nd}$ (0.41–0.64). The uniform isotopic values measured at Tshibinda contrast with the wide ranges recorded in other parts of the volcanic province. Lavas from the earliest phase of mafic volcanism in the Kivu Bukavu group have $^{87}Sr/^{86}Sr$ values between 0.70314 and 0.70493 and $\varepsilon_{Nd}$ between 2.17 and 7.57 (Fig. 6). The 13 remaining lavas, of all ages and from throughout the Kivu area, fall within this isotopic range and do not show a consistent geographic variation.

Several ratios of incompatible trace element abundances correlate negatively with Nd isotopic values (e.g., Th/Nb, La/Nb, Ba/Nb), suggesting that they — like Sr isotopic ratios — are a feature of the mantle source region and vary over short distances. In each case, lavas from Tshibinda form an endmember in the Kivu suite.

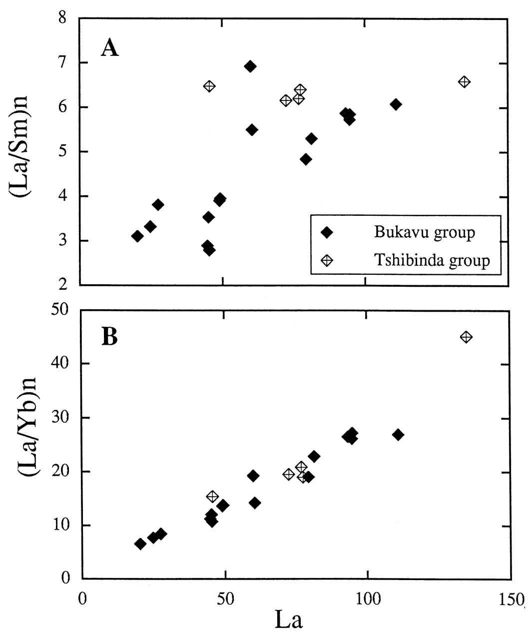


Fig. 5. (A) $(La/Sm)_n$ vs. La abundance for Kivu mafic lavas. (B) $(La/Yb)_n$ vs. La. The large variations in MREE abundances are manifest in a narrow range in LREE/MREE ratios that do not vary with La content, but values of LREE/HREE that are positively correlated with La abundances.

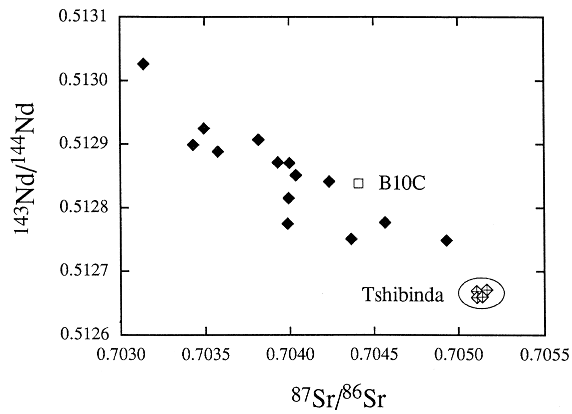


Fig. 6. $^{87}Sr/^{86}Sr$ vs. $^{143}Nd/^{144}Nd$ for Kivu mafic lavas. Sr and Nd isotopes are negatively correlated among all Kivu lavas. Samples from Tshibinda (circled) have a restricted compositional range, while samples from the remainder of the Kivu province show a high degree of variability. Sample B10C from Burundi is indicated by an open square.

## 3. Discussion

### 3.1. Major element characteristics of mafic rift lavas

The eastern and western branches of the rift system are characterized by differences in the timing, volume and chemical composition of erupted lavas. In the eastern rift, volcanism began at roughly 23 Ma and the total erupted volume is estimated at 220,000 $km^3$ (Williams, 1972). The Kenya rift volcanics erupted nearly continuously from Early Miocene to Holocene time (Baker et al., 1971). In general, the Kenya basalts are weakly undersaturated with respect to silica. Erupted compositions considered in this study include tholeiites, ferrobasalts and alkali basalts from Ol Tepesi and Naivasha in central Kenya (Baker et al., 1977; Davies and Macdonald, 1987), and alkali basalts and basanites from Huri Hills in northern Kenya (Class et al., 1994). Lavas from northern Tanzania (Paslick et al., 1995) are dominated by mildly alkalic compositions and include samples from several volcanic vents that date from $>8$ Ma to Recent.

Volcanism in the western rift began at roughly 12 Ma and has produced at most 100,000 $km^3$ of lava (Kampunzu and Mohr, 1991). Eruptions have been restricted to four volcanic provinces (Fig. 1) located in heavily faulted intrabasinal accommodation zones (e.g., Ebinger, 1989a,b). Mafic lavas from the western rift are undersaturated with respect to silica, although the nature and degree of alkali enrichment vary greatly both within and between volcanic provinces. Toro Ankole is dominated by ultrapotassic lavas and other highly alkaline compositions, including pyroclastic carbonatites (e.g., Holmes and Harwood, 1937; Lloyd and Bailey, 1975; Lloyd et al., 1991). The Virunga lavas are mildly to highly undersaturated, with compositions ranging from alkali basalts to K-rich (ultrapotassic) basanites (Holmes and Harwood, 1937; De Mulder et al., 1986; Marcelot et al., 1989; Rogers et al., 1992, 1998). Kivu province lavas are similar to eastern rift compositions, including alkali basalts and the only tholeiitic lavas sampled in the western rift (Kampunzu et al., 1986; Auchapt et al., 1987; Marcelot et al., 1989). To the south, Rungwe lavas include alkali basalts, basanites, nephelinites, as well as the only trachy-phonolitic central volcanoes in the western rift (Harkin, 1960; Furman, 1995). In the following discussion, we consider lavas from each of these volcanic provinces.

### 3.2. REE characteristics of mafic rift lavas

We begin with the REE because the composition of mantle peridotite can be used as a well-defined reference point, and because REE behavior during melting is reasonably well-understood. Chondrite-normalized diagrams for all volcanic provinces of the East African Rift system show LREE enrichments relative to HREE (Fig. 7). In most cases (e.g., Virunga province in the western rift and Naivasha and Ol Tepesi from the eastern rift), lavas from a single area have sub-parallel REE patterns that do not cross one another, and REE abundances that increase as MgO contents decrease. Lavas from Rungwe and the Katwe-Kikorongo field of Toro Ankole in the western rift, plus Huri Hills in the eastern rift, display minor heterogeneity indicated by a small number of REE patterns that vary primarily in their abundances of Tb through Lu. In contrast, lavas from the Kivu province are markedly heterogeneous in relative abundances of all the REE.

Among mafic lavas from all volcanic areas, the degree of LREE-enrichment, and the overall steepness of the sloping REE patterns (Fig. 7) generally increase together, as well as increasing with degree of silica undersaturation. The range of $(La/Sm)_n$ values among basalts, alkali basalts and ferrobasalts from Naivasha, Ol Tepesi, and Huri Hills (2.2–3.5) is somewhat smaller than the range observed among Huri Hills basanites (3.0–4.5) or at any single western rift volcanic center. In the western rift $(La/Sm)_n$ values at Rungwe, Karisimbi and Muhavura overlap (4.0–5.5), while values at Nyiragongo (5.2–6.7) and Toro-Ankole (6.0–6.7) are markedly higher. Notably, lavas from the Kivu province show the widest range in $(La/Sm)_n$ values (3.0–7.0). In this province, basalts from the Bukavu group have similar values to the eastern rift (3.0–4.0), while lavas from the Tshibinda group have values similar to Nyiragongo and Toro-Ankole lavas (5.6–7.0). Lavas with relatively uniform $(La/Sm)_n$ values from Kivu, Nyiragongo and Toro-Ankole have very different $(La/Yb)_n$ values. Based on the extremely wide range

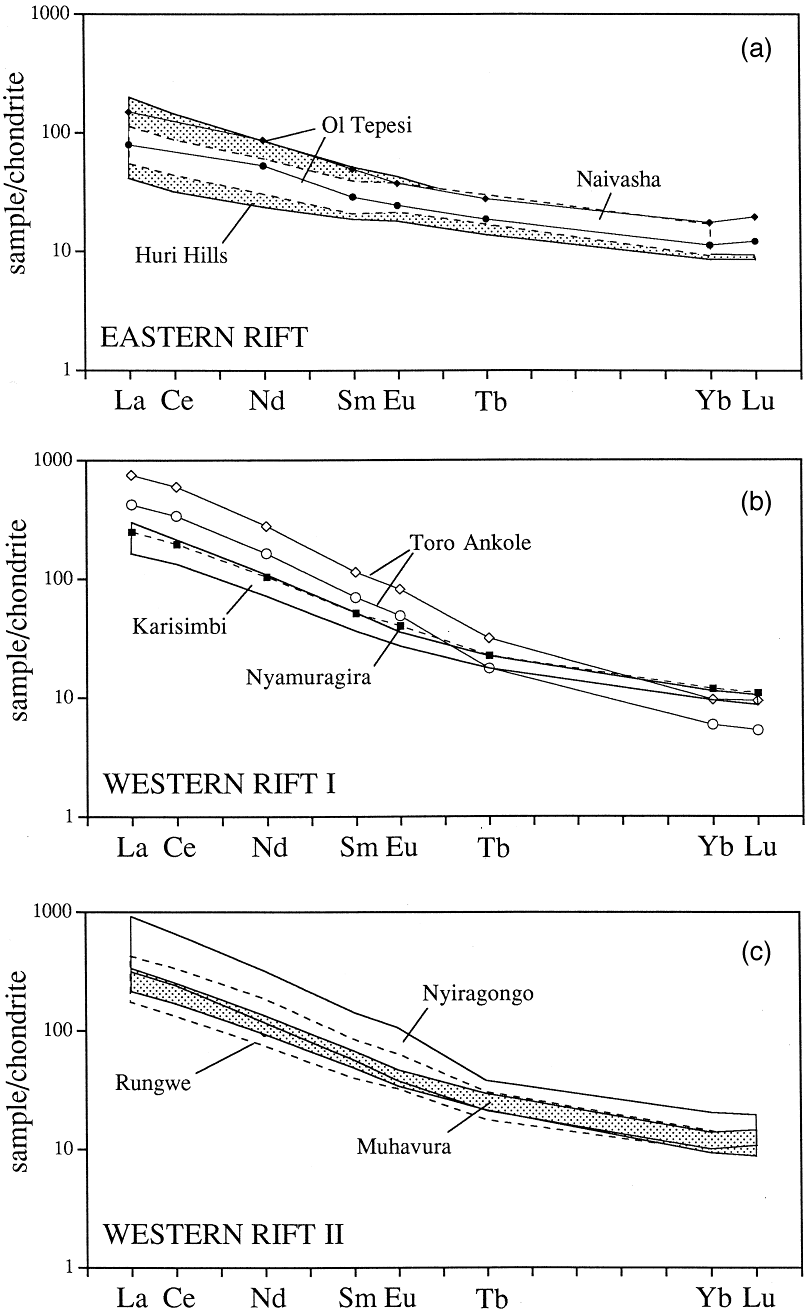


Fig. 7. Chondrite-normalized abundances of REE (values of Boynton, 1983). Datasets were chosen on the basis of internal consistency when possible (data from same analytical facilities), and therefore do not include all available published data. Sources of data: Huri Hills — Class et al. (1994); Naivasha — Davies and Macdonald (1987); Ol Tepesi — Baker et al. (1977); N. Tanzania — Paslick et al. (1995); Muhavura — Rogers et al. (1998); Karisimbi — Rogers et al. (1992); Rungwe — Furman (1995); Nyiragongo — Marcelot et al. (1989), Furman (unpublished data); Toro Ankole — Furman (unpublished data). (a) Eastern rift lavas. Ranges shown enclose the variation among mafic lavas from Ol Tepesi, Naivasha and Huri Hills. (b) Western rift I. The field for Karisimbi encompasses all primitive K-basanites. Two samples from Toro Ankole and one mafic lava from Nyamuragira were selected to indicate representative patterns in these areas. (c) Western rift II. Fields for Muhavura, Nyiragongo and Rungwe indicate the range of mafic lavas from each area.

in REE patterns, Mitchell and Bell (1976) concluded that the Toro-Ankole lavas, especially the ultra-alkaline ugandites, mafurites and katungites, could not be derived by a single-stage melting process from mantle peridotite, but require at least one earlier event of source enrichment.

### *3.3. Incompatible trace and minor element variations*

Incompatible trace elements may give useful insight into the interaction between magmas derived from asthenospheric and lithospheric sources. In particular, they can indicate the type of mantle involved (e.g., HIMU), the existence or extent of contamination by crust, the nature and degree of metasomatic enrichment events, and the source mineralogy when elements diagnostic of key phases such as apatite, zircon, or phlogopite are considered.

All volcanic areas show enrichment in the highly incompatible elements relative to MORB and OIB, and the primitive-mantle normalized patterns (spidergrams) are not smooth (Fig. 8). Lavas from the

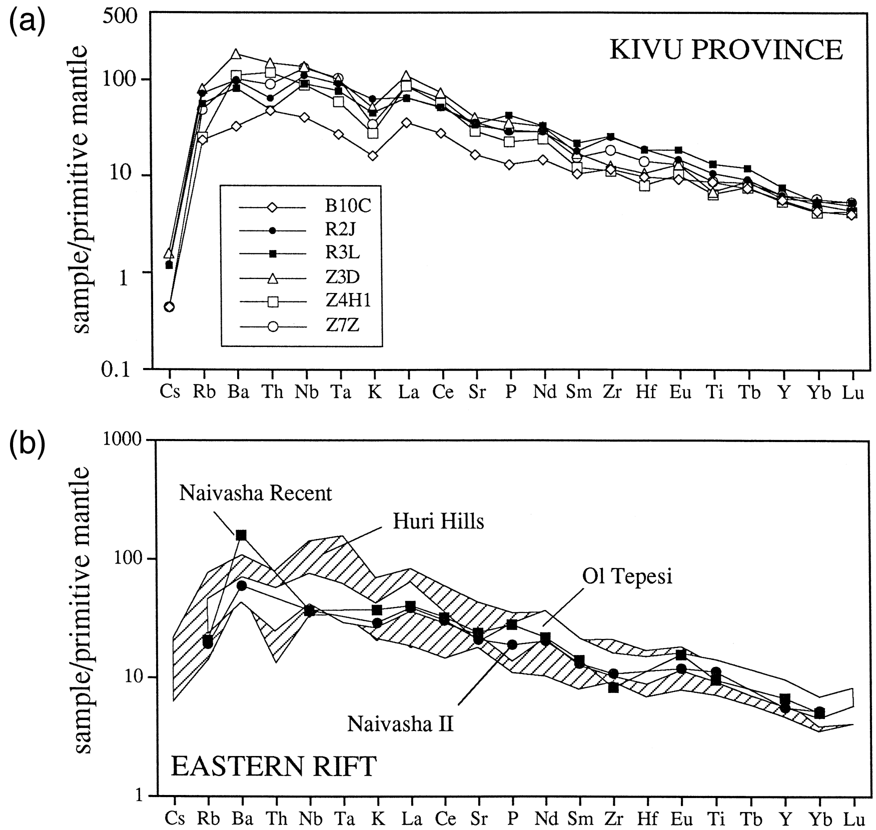


Fig. 8. Primitive mantle normalized incompatible element variation diagrams for mafic rift volcanics (normalizing values of Sun and McDonough, 1989). See text for discussion. (a) Kivu province. Mafic lavas from the Tshibinda and Bukavu groups have distinct patterns; note particularly the differences in Ba–Th and K–La between the two groups. One sample from Burundi has the lowest incompatible trace element abundances of all Kivu lavas. (b) Eastern rift lavas. Ranges shown enclose the variation among mafic lavas from Ol Tepesi and Huri Hills. Two representative samples from Naivasha indicate the distinct trace element abundances of mafic lavas from different ages and/or eruptive centers. (c) Western rift I. The field for Karisimbi encompasses all primitive K-basanites. Two samples from Toro Ankole and one mafic lava from Nyamuragira were selected to indicate representative patterns in these areas. (d) Western rift II. Fields for Muhavura and Rungwe indicate the range of mafic lavas from these areas. One representative nephelinite from Nyiragongo is shown for comparison.

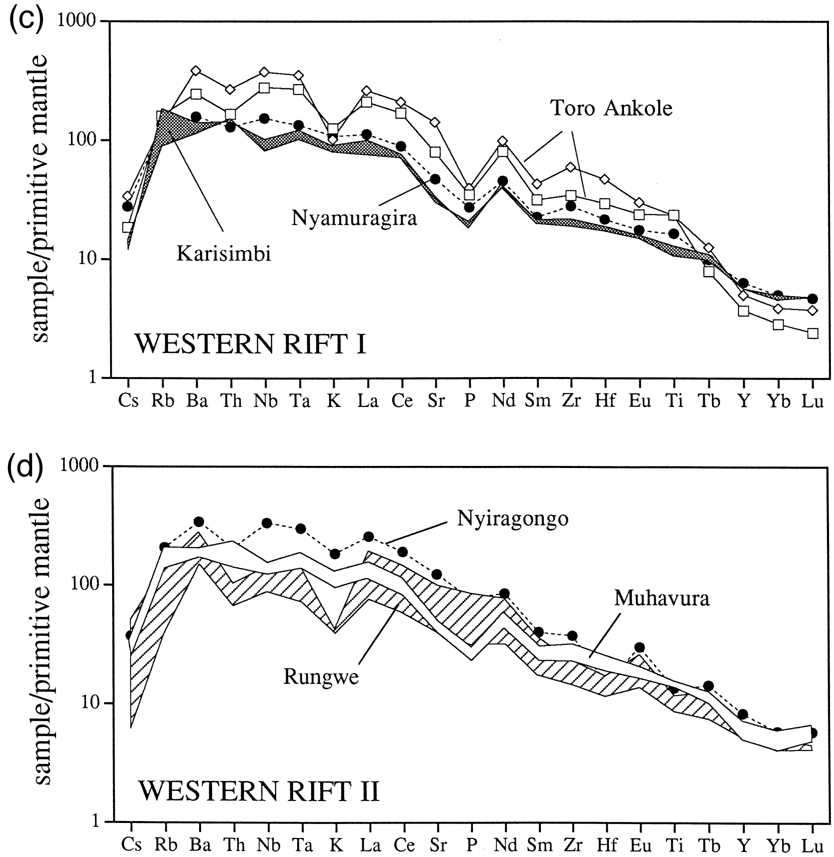


Fig. 8 (continued).

eastern rift display smoother overall spidergram patterns, and have lower incompatible trace element abundances, than those from the western rift. In general, lavas from a single area have parallel spidergrams; as discussed earlier, the Kivu province is exceptional in this regard. As expected on the basis of REE variations, lavas from all western rift volcanoes (except the Bukavu group from Kivu) show steep to concave-upward patterns from Ti to Lu (Fig. 8), with limited abundance ranges for these elements. Among eastern rift lavas, this pattern is seen only for the Huri Hills basanites. This signature is indicative of melting in the presence of residual garnet, a phase in which these elements are compatible.

Mafic rift lavas generally show no evidence of crustal contamination. These mafic lavas have unusually high abundances of incompatible trace elements which make them unlikely to be contaminated easily during ascent or in crustal chambers. Detailed arguments regarding the lack of crustal assimilation have been made by several authors (e.g., Baker et al., 1977; Davies and Macdonald, 1987; Marcelot et al., 1989; Rogers et al., 1992, 1998; Class et al., 1994; Furman, 1995) and will not be presented here. As one example, values of Sr/Ce are within the range of ocean island basalts ($\sim$ 5–8) for lavas from all provinces in the western rift, and are slightly higher (9–12) in lavas from Huri Hills and Naivasha. Lavas that have assimilated continental crustal material should have elevated values of Sr/Ce and positive Eu anomalies resulting from incorporation of plagioclase feldspar. Rift lavas do not have these signatures, and thus the Sr/Ce values are characteristic features of their source regions. As similar arguments can be made for other individual elements, we infer that the incompatible trace element features of mafic rift lavas have not been affected by crustal assimilation and can be used to fingerprint the source region.

### 3.3.1. Regional patterns of incompatible trace element enrichment

There are key similarities throughout the rift system in the covariations of certain incompatible elements such as K, Ba, Rb, Th, Nb and La. Consistent geographic patterns of anomalous enrichment and depletion suggest that regional mineralogical heterogeneities in the underlying lithospheric mantle control the distribution of these anomalies in the erupted lavas.

The most obvious feature of the spidergrams is the large negative potassium anomalies in lavas from Kivu (Bukavu group), Rungwe and Toro Ankole in the western rift, and from Naivasha in the eastern rift (Fig. 8). The degree of relative K depletion does not correlate with the level of incompatible trace element abundances (cf. Rungwe and Muhavura; Fig. 8) or with potassium content of the lavas (cf. Toro Ankole and Muhavura; Fig. 8). Relative potassium depletion is, however, correlated with Ba enrichment (Fig. 8). Ba enrichment is reflected in Ba/Rb values higher than the primitive mantle estimate of ~ 11 (Sun and McDonough, 1989) in samples from the Kivu Bukavu group, Toro Ankole, Rungwe, Nyamuragira, Nyiragongo and all eastern rift localities. Individual lavas from Rungwe, Naivasha, Ol Tepesi and Huri Hills have Ba/Rb values ranging from ~ 18 to over 100. Note that the Tshibinda group alkali basalts and ultrapotassic lavas from Karisimbi and Muhavura do not show Ba enrichment or K depletion.

Covariation between Nb and Th illustrates the same regional pattern in trace element enrichment. Samples from the Kivu Tshibinda group, Karisimbi, and Muhavura have Nb/Th values close to the estimated primitive mantle value of ~ 8 (Sun and McDonough, 1989). In contrast, samples from the Kivu Bukavu group, Rungwe, Toro Ankole, Ol Tepesi and Huri Hills have Nb/Th values ~ 12, and indicate a higher compatibility for Th in the mantle source beneath these areas.

Patterns of variation in Ba/Nb–La/Nb also suggest involvement of several source regions with distinct enrichment histories. Samples from the Kivu Bukavu group and Toro Ankole have Ba/Nb ratios similar to primitive mantle estimates (~ 10; Sun and McDonough, 1989) but La/Nb ratios between 0.6 and 0.9, lower than primitive mantle values (~ 0.96; Fig. 9). In contrast, mafic lavas from the Kivu Tshibinda group and Muhavura have La/Nb ratios similar to primitive mantle but have higher Ba/Nb ratios (12–14). Huri Hills basanites have Ba/Nb–La/Nb ratios that overlap the field of HIMU mantle inferred from ocean island basalt (Weaver, 1991; Fig. 9). Rungwe nephelinites and Karisimbi K-basanites have large ranges in Ba/Nb and La/Nb, and form trends suggesting involvement of an enriched mantle (EMII) component, while alkali basalts from Rungwe and Naivasha are relatively enriched in Ba and trend towards EMI mantle. Alkali basalts from Huri Hills and Ol Tepesi are also enriched in Ba, and show increasing Ba/Nb ratios at constant La/Nb (Fig. 9). These variations are characteristic of enriched mantle reservoirs identified for OIB, but we suggest that they are present within the continental lithosphere as well.

### 3.3.2. Evidence for carbonatite metasomatism

A diagnostic feature of metasomatized mantle is an increase in Zr/Hf value (Dupuy et al., 1992; Rudnick et al., 1993), with values ranging between ~ 45 and 100. All rift samples have higher Zr/Hf values than the primitive mantle (~ 36; Sun and McDonough, 1989): average Zr/Hf values for Toro Ankole, Muhavura, Karisimbi and the eastern rift provinces range from 41–45. The elevated Zr/Hf (and overall high trace element abundances) suggest that small-volume metasomatic fluids have enriched the source regions for every province. Lavas from the Kivu Tshibinda group, Rungwe and Nyiragongo have the highest Zr/Hf values, with individual samples from these provinces between 60–83. These same regions show enrichment in REE relative to HFSE (e.g., Eu/Ti; Fig. 8). Both of these signatures are characteristic of carbonatite metasomatism (Dupuy et al., 1992; Rudnick et al., 1993) and suggest that the source areas for these mafic lavas were infiltrated by carbonate-rich magma. The geographic distribution of this source signature differs from that just described on the basis of other incompatible trace elements, and suggests that portions of

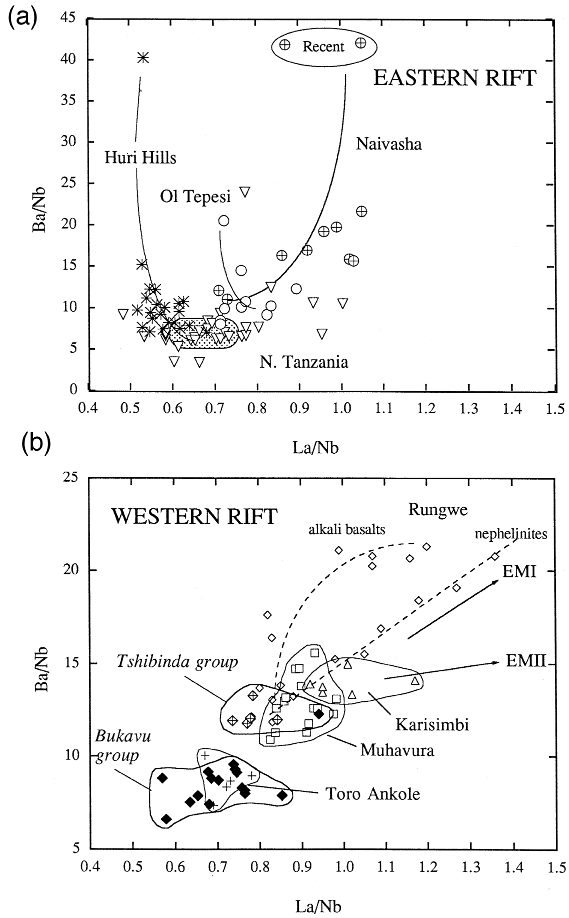


Fig. 9. Ba/Nb against La/Nb for East African rift volcanics. (a) Eastern rift lavas have generally lower Ba/Nb and La/Nb values than primitive mantle estimates (Sun and McDonough, 1989), but each volcanic center includes samples with extremely high Ba/Nb values. Huri Hills basanites overlap estimates for HIMU (Weaver, 1991), consistent with their inferred plume source (Class et al., 1994). (b) Western rift lavas from the Tshibinda and Bukavu groups at Kivu have distinct ranges in Ba/Nb–La/Nb that indicate a sharp discontinuity in source composition between the two areas. Bukavu group samples overlap those from Toro Ankole and are depleted relative to primitive mantle estimates. Tshibinda group Kivu and Muhavura lavas, as well as individual samples from Rungwe and Karisimbi, have overlapping ranges in Ba/Nb–La/Nb (10–14 and 0.8–0.9, respectively) that are similar to values observed at Naivasha. This range is interpreted to represent the range in the CLM source region. Primitive K-basanites from Karisimbi trend from the CLM source towards the EMII endmember, while Rungwe nephelinites trend towards EMI. Rungwe alkali basalts are enriched in Ba relative to associated nephelinites, probably due to an increased importance of amphibole melting in their mantle source region, and they trend towards the high values observed in the eastern rift.

the lithosphere beneath the rift branches underwent more than one phase of metasomatic enrichment.

### *3.4. Sr–Nd isotopic characteristics of East African Rift mafic lavas*

In this section we focus on the Sr and Nd isotopes because these data provide constraints on mantle source compositions and they are available for a wide range of lava types from both rift branches. We begin by summarizing the Sr–Nd isotopic relations of East African carbonatites and associated undersaturated mafic lavas, because they are central to a comprehensive model of regional magnetism.

The East African Carbonatite Line (EACL) was defined by Bell and Blenkinsop (1987) on the basis of Sr–Nd isotopic variations for young carbonatite lavas (Fig. 10). The principle carbonatite localities defining the EACL are eastern Uganda (Kisingiri, Napak, Tororo, Sukulu), western Uganda (Kalyango, Rusekere), northern Tanzania (Oldoinyo Lengai) and Kenya (Homa Bay). The EACL has been interpreted as a mixture between two mantle sources (Bell and Blenkinsop, 1987), with compositions similar to some ocean island basalt sources (Nelson et al., 1988), notably the HIMU (high U/Pb) and EMI (enriched mantle type 1) components (as described by Zindler and Hart, 1986). Diopsides from South African kimberlites (Menzies and Murthy, 1980) overlap the EACL at low $\varepsilon_{Nd}$ compositions and, notably, they form an extension of the array to much more enriched values ($\varepsilon_{Nd} = -13$, $^{87}Sr/^{86}Sr = 0.7075$; Fig. 10). Although these kimberlites are located well outside the area of study for this paper, they demonstrate that the processes giving rise to the isotopic variations in the East African region are of general significance in the evolution of the SCLM. Recent isotopic studies at individual carbonatite localities have revealed significant isotopic heterogeneity (e.g., Kalt et al., 1997), including some samples that do not fall along the EACL but rather are offset from it, to higher $^{87}Sr/^{86}Sr$ or $^{143}Nd/^{144}Nd$ (Fig. 10). Collectively, the isotopic data demonstrate that large ranges in isotopic composition are present, often over very short distances, within the East African lithospheric mantle.

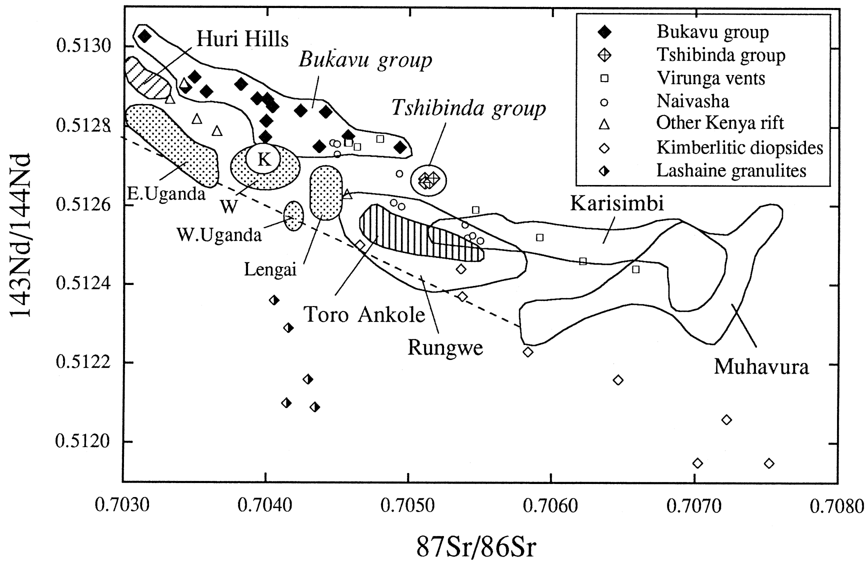


Fig. 10. $^{143}Nd/^{144}Nd$ vs. $^{87}Sr/^{86}Sr$ for selected lavas, carbonatites and xenoliths from East Africa. Results for Kivu lavas analyzed in this study are shown by diamonds, separated into Bukavu and Tshibinda groups. Fields for other western rift lavas include Rungwe nephelinites and alkali basalts (Graham et al., in prep.), Toro Ankole lavas and xenoliths (Davies and Lloyd, 1989; Graham et al., in prep.), Karisimbi basanites and potassic basanites (Rogers et al., 1992), Muhavura potassic hawaiites and basanites (Rogers et al., 1998), and undersaturated mafic lavas from small vents and cones in the Virunga province (Vollmer and Norry, 1983). Eastern rift lavas include Naivasha basalts shown by open circles (Davies and Macdonald, 1987) and other lavas from Kenya shown by open triangles (Norry et al., 1980). The field for Huri Hills basanites and alkali basalts is from Class et al. (1994). Stippled fields show carbonatites from the eastern rift; E. Uganda (Tororo, Busuku, Napak and Sukulu; Bell and Blenkinsop, 1987; Nelson et al., 1988); W — Wasaki peninsula (Kalt et al., 1997), Oldoinyo Lengai (Bell and Simonetti, 1996), K — Kerimasi, N. Tanzania (Kalt et al., 1997). The dashed line is the EACL from Bell and Blenkinsop (1987). Granulite xenoliths from Lashaine, Tanzania are from Cohen et al. (1984), and open diamonds show diopsides from South African kimberlites (Menzies and Murthy, 1980).

Mafic lavas from the eastern and western rift branches define an elongate Sr–Nd isotope array that, to a first approximation, lies parallel to the EACL source (Fig. 10). The isotopic variations in these mafic lavas are clearly decoupled from variations in key trace element ratios that are indicative of crustal contamination, such as Ce/Pb, and therefore, they must primarily be source region features.

Despite the isotopic variability, we can identify consistent regional patterns for lavas from both the eastern and western rift branches. The high $\varepsilon_{Nd}$ values and low $^{87}Sr/^{86}Sr$ observed at Kivu are similar to some oceanic basalts, suggesting a sub-lithospheric source. The isotopically more enriched (low $\varepsilon_{Nd}$) Kivu lavas from Tshibinda volcano trend towards the enriched compositions found in the East African Rift system, such as the primitive-K basanites from Karisimbi (Rogers et al., 1992). The western Virunga vents of Nyiragongo, Goma and Bushwaga also have isotopic compositions that lie within the Kivu array, whereas mafic lavas from the eastern Virunga volcanoes Karisimbi, Visoke and Muhavura are the most highly enriched lavas for which crustal contamination cannot be demonstrated (Rogers et al., 1992, 1998). More evolved lavas from this area, such as the Sabinyo quartz latites (Vollmer and Norry, 1983), clearly show the effects of crustal contamination, and we have not considered them in the discussion. Isotopic compositions intermediate to these extremes are found at isolated vents in central Virunga (Muganza, Busamba, Mukuyu and Mikeno localities; Vollmer and Norry, 1983). Taken together, lavas from the Kivu and Virunga provinces define a broad Sr–Nd isotope array, termed here the K–V array. The Sr and Nd isotope compositions of a lava along the K–V array correspond roughly to its geographic position: lavas from Tshibinda have isotope compositions overlapping those of western

Virunga, whereas lavas from the Bukavu group have lower $^{87}Sr/^{86}Sr$ and those from eastern Virunga have higher $^{87}Sr/^{86}Sr$ (Fig. 10).

Sr and Nd isotopic analyses for mafic lavas from Rungwe, and lavas and xenoliths from the Toro-Ankole province (Davies and Lloyd, 1989; Graham et al., in preparation) define smaller clusters located between the EACL and the K–V array. Rungwe nephelinites and basanites show a near-horizontal Nd–Sr trend very much like lavas from Toro-Ankole, while Rungwe alkali basalts lie close to the EACL, but are displaced slightly towards the K–V array. While the isotopic data for both the Toro-Ankole and Rungwe suites clearly show that their source regions are heterogeneous, the range of variation is much smaller than that observed in the Kivu and Virunga provinces, and it does not correspond in any simple way to geographic location.

Lavas from the eastern branch of the rift have Sr and Nd isotope compositions that overlap both the K–V array and the range of Rungwe and Toro-Ankole lavas. Lavas from Huri Hills show lower $^{87}Sr/^{86}Sr$ for a given $^{143}Nd/^{144}Nd$ as compared to the Kivu province, and lie near the most depleted (high $\varepsilon_{Nd}$) part of the K–V array (Fig. 10). Among the Naivasha suite, the oldest Pleistocene lavas plot along the K–V array with compositions similar to Nyiragongo and its adjacent vents (Davies and Macdonald, 1987). Later Pleistocene basalts (Naivasha II in Fig. 10) plot among the highest $^{87}Sr/^{86}Sr$ samples from Rungwe and Toro Ankole, while Recent Naivasha basalts have isotopic values that fall between the other two age groups. Mafic lavas from northern Tanzania (Paslick et al., 1995) show a range in Sr–Nd isotopes similar to that observed at Naivasha (Fig. 10). Notably, two lavas from Essimingor span the entire range ($\varepsilon_{Nd} = 2.4$ to $-4.9$), again indicating a source region that is heterogeneous on a short length scale.

### 3.5. Isotope and trace element characteristics of lithospheric mantle sources

The extreme Sr–Nd isotopic variability of East African Rift lavas requires melting of heterogeneous mantle sources dominantly located in the continental lithospheric mantle (e.g., Vollmer and Norry, 1983; Rogers et al., 1992, 1998; Williams and Gill, 1992). Despite this isotopic variability, western rift lavas show a convergence in Sr $\simeq$ Nd $\simeq$ Pb isotopes near values of $^{87}Sr/^{86}Sr \sim 0.7050$, $^{143}Nd/^{144}Nd \sim 0.51264$ ($\varepsilon_{Nd} \sim 0$) and $^{206}Pb/^{204}Pb \sim 19.0$ (Graham et al., 1995). The isotopic convergence is defined by a relatively small range of common values found at all western rift and some eastern rift volcanoes. The full range in values for individual provinces extends away from this convergence to distinct compositions characteristic of each area. We observe this convergence among selected lavas from Kivu and Rungwe (data from this study and Graham et al., in preparation), Toro Ankole (Davies and Lloyd, 1989; Graham et al., in preparation), Karisimbi and Muhavura (Rogers et al., 1992, 1998), Naivasha (Davies and Macdonald, 1987) and northern Tanzania (Paslick et al., 1995). Each volcanic province examined, except Huri Hills, has some samples with $^{87}Sr/^{86}Sr \sim 0.7050$ and $^{143}Nd/^{144}Nd \sim 0.51264$ ($\varepsilon_{Nd} \sim 0$) (Fig. 10). Mafic lavas from Rungwe and Toro Ankole show a restricted range and lie near the convergence in Sr and Nd isotopes, extending slightly towards the EACL. In contrast, other volcanic areas that display a large isotopic range, including Kivu, Karisimbi, Muhavura, Naivasha and northern Tanzania, define distinct trends in Sr–Nd isotopes that radiate away from the convergence in isotope composition rather than straddling it. This pattern suggests to us that a CLM source having isotope compositions near this convergence is available beneath each of these volcanic areas. The CLM source may, however, be intimately mixed (laterally or vertically) with other source materials having different isotope compositions, and these may be distinct for each volcanic area.

Within each volcanic area, many incompatible trace element ratios vary as a function of lava type and/or Sr–Nd isotopic composition (Marcelot et al., 1989; Rogers et al., 1992, 1998; Class et al., 1994; Furman, 1995). Thus, the trace element variations for individual areas typically reflect small-scale intermingling of distinct sources or their derivative melts. Considering the eastern and western rift datasets together, there are certain incompatible trace element ratios, such as La/Nb and Ba/Nb, which overlap among several sample suites, and which also show characteristics consistent with a CLM source identified from Sr–Nd isotopes. Variations in La/Nb,

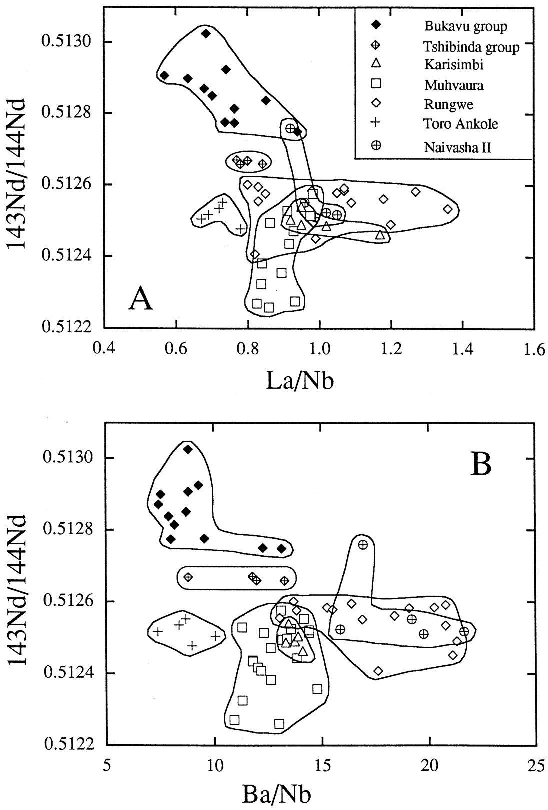


Fig. 11. Relationships between $^{143}Nd/^{144}Nd$ and incompatible trace element ratios. These variations allow a characterization of the CLM source. Lavas from the Tshibinda group at Kivu, Muhavura, Karisimbi, Rungwe, Toro Ankole and Naivasha define trends that converge at a narrow range of values. See text for full discussion. (A) La/Nb–$^{143}Nd/^{144}Nd$. (B) Ba/Nb–$^{143}Nd/^{144}Nd$

Ba/Nb and Nb/Th against $^{143}Nd/^{144}Nd$ (Fig. 11) reveal a small field of overlapping values among samples from Kivu (Tshibinda), Karisimbi, Muhavura, Rungwe, Toro Ankole and Naivasha. Trends for each volcanic province have different slopes and orientations, but they converge at a common area. Like the Sr–Nd–Pb isotope systematics described by Graham et al. (1995), overlap does not occur at a single value but rather requires a small range and, by inference, some degree of isotopic and trace element heterogeneity in the CLM source.

### 3.6. Mineralogy of the lithospheric mantle source

An accurate knowledge of the source mineralogy for lithospheric melts can place important constraints on the thermal structure of the subcontinental mantle. In the case of the African Rift system, variations in the depth of melting along and across the rift axes may be used to infer the degree of asthenospheric upwelling and hence, the three-dimensional shape of the plume head. A general picture of the shape of the plume is available from detailed geophysical studies (e.g., Simiyu and Keller, 1997), but the presence of mineralogical barometers such as garnet, amphibole and phlogopite in the source region for mafic rift lavas offers an increase in resolution of the shallow lithospheric structure, and ultimately, it can provide estimates of the rate of lithospheric erosion or thinning. We note that the low estimates of crustal extension across, in particular, the western rift (< 15%, Ebinger, 1989b), favor a model of lithospheric erosion rather than one of extensional thinning. In this section, we outline the inferred source mineralogy along both rift branches, identifying features of the CLM source as well as those of other parts of the lithospheric mantle that contribute to African rift volcanism.

Several lines of evidence suggest that garnet is present in the source regions of most western rift mafic lavas. The high $(La/Yb)_n$ values and the concave-upward spidergrams (Fig. 8) of lavas from the Kivu Tshibinda group, Rungwe, Toro Ankole, Karisimbi, Muhavura and Nyiragongo indicate that the HREE are more compatible than LREE and MREE in the source residue. This feature is also present in some, but not all, of the Bukavu group lavas from Kivu. Furman (1995) used a REE inversion model to infer that melting at Rungwe occurs within the spinel–garnet transition zone (~60–80 km). REE abundances and $(La/Yb)_n$ values at Muhavura that are similar to those at Rungwe led Rogers et al. (1998) to infer a comparable melting depth beneath eastern Virunga. In eastern rift lavas, the geochemical evidence for residual garnet in the mantle source is more equivocal, as high $(La/Yb)_n$ values are found only in Huri Hills basanites. HREE abundances in lava suites from Ol Tepesi and Naivasha are markedly more variable than those from the western rift volcanoes. Spinel- and garnet-bearing lherzolite xenoliths found at Marsabit in northern Kenya and the Chyulu volcanic field in southern Kenya (Henjes-Kunst and Altherr, 1992) suggest that melting occurs at or below the depth where garnet becomes stable in these areas. These sites are both located east of the main rift and may record different melting processes than those beneath the rift axis.

Relative abundances of the alkali and alkaline earth elements can be used to assess the presence of amphibole and/or phlogopite in the mantle source region. These phases are important because they can attest to the metasomatic enrichment history of the source region, as well as helping to constrain the depth of melting. Both Rb and Ba are compatible in phlogopite (LaTourette et al., 1995), while Rb, Sr and Ba are moderately compatible in amphibole (Adam et al., 1993; LaTourette et al., 1995). Melts in equilibrium with phlogopite are expected to have significantly higher Rb/Sr and lower Ba/Rb values than those formed from amphibole-bearing sources. Conversely, melts of an amphibole-bearing source may have extremely high Ba contents and Ba/Rb values.

Several lines of evidence suggest that ultrapotassic lavas from Toro Ankole, Karisimbi and Muhavura formed through melting of a phlogopite-bearing lithospheric mantle source. These lavas have high Rb/Sr ($> 0.10$) and low Ba/Rb values ($< 20$) (Fig. 12). They also incorporate micaceous xenoliths (Holmes and Harwood, 1937; Lloyd and Bailey, 1975; Davies and Lloyd, 1989; Lloyd et al., 1991) and/or phlogopite xenocrysts (Rogers et al., 1998). Experimental stability estimates for phlogopite-bearing assemblages suggest melt formation at pressures near 30–35 kbar, or depths of 90–100 km (Olafsson and Eggler, 1983; Wallace and Green, 1988; Lloyd et al., 1991; Sato et al., 1997). In contrast, lavas from many volcanic areas have low $K_2O/Na_2O$ ($< 0.75$) and low Rb/Sr values ($< 0.06$, Fig. 12), consistent with melting of an amphibole-bearing source. Tshibinda group lavas from Kivu have higher Rb/Sr values than Bukavu group lavas with similar Ba/Rb values, suggesting that a small amount of phlogopite may have been present in the source prior to the onset of melting beneath this area. It is also significant that low-MgO mafic lavas from Muhavura, Karisimbi and Toro Ankole have Ba/Rb–Rb/Sr values that overlap those of the Tshibinda group.

We suggest that the CLM source is a spinel–garnet lherzolite containing small amounts of amphibole and/or phlogopite and perhaps other minor, metasomatic phases. Dawson and Smith (1988, 1992) describe xenoliths from northern Tanzania that contain both amphibole and phlogopite, and suggest that they result from metasomatic infiltration by ultra-alkaline katungite lava. These observations suggest a widespread enrichment event beneath both the eastern and western rift branches, although a common timing remains to be demonstrated. A small number of alkali basalts from Huri Hills, Naivasha, Ol Tepesi, Rungwe and northern Tanzania have high Ba/Rb values ($> 50$, Fig. 12) that suggest melting of amphibole-bearing (phlogopite-free) lherzolite. In all cases, these samples appear to be contemporaneous with lavas derived from the CLM source. On a local scale, it is difficult to distinguish differences in the history of metasomatic enrichment from differences in phase stability structure of the underlying lithospheric mantle. We therefore suggest that the eruption of lavas closely spaced in time, but derived from mantle regions having very different source mineralogy, is most simply explained by melt generation over a range of depths beneath each volcanic province.

The minor phase mineralogy of the CLM source is difficult to constrain and, indeed, may vary on a very short spatial scale (Furman, 1995). In this study, values of Nb/Th correlate negatively with Rb/Sr (Fig. 12) and hence, positively with Ba/Rb (not shown). This relationship is apparent both within and between suites of lavas, and suggests that the Nb/Th systematics of erupted melts may also be controlled by the source mineralogy. We suggest two interpretations that are consistent with the observed regional trends, and that may help further constrain the CLM source mineralogy. First, because Nb is more compatible in amphibole than in phlogopite (LaTourette et al., 1995; Ionov et al., 1997), the progressive removal of phlogopite from amphibole + phlogopite could produce the observed variations. Second, oxide minerals that form during alkali-rich metasomatism may control Nb abundances throughout the melting process (Ionov et al., 1999). Additional work on xenolith suites may prove essential to resolving this question.

Class and Goldstein (1997) have discussed evidence for the presence of amphibole and phlogopite in the mantle sources for some ocean island basalts,

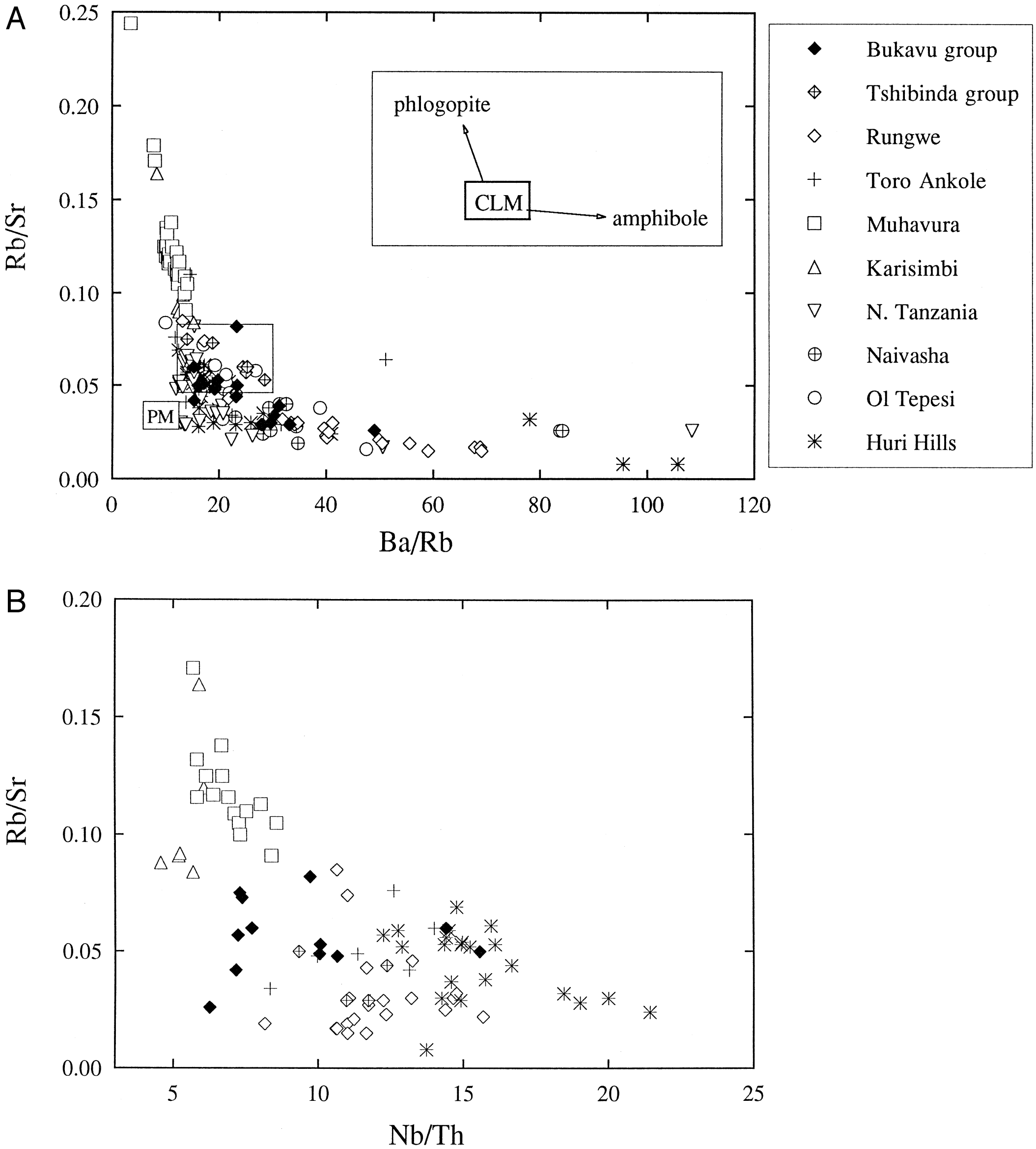


Fig. 12. Variations in incompatible trace element ratios that may constrain source mineralogy. (A) Rb/Sr vs. Ba/Rb. The mineralogy of the CLM source is inferred to include minor amounts of both amphibole and phlogopite. The field indicated that CLM was drawn to enclose samples identified to have been derived from the CLM source on the basis of isotopic and trace element relationships (see text). High Rb/Sr and Ba/Rb values of all rift samples relative to primitive mantle estimates (PM; Sun and McDonough, 1989) appear to require a widespread enrichment (metasomatic) event. Extremely high Rb/Sr values at Toro Ankole, Muhavura and Karisimbi indicate a greater importance of phlogopite melting in the lithospheric mantle source, whereas high Ba/Rb among eastern rift lavas and Rungwe alkali basalts indicate phlogopite-absent melting of amphibole lherzolite. The amphibole-rich source likely results from carbonatite metasomatism in some cases, whereas abundant phlogopite suggests a relatively higher $H_2O/CO_2$ ratio in the metasomatic agent. (B) Rb/Sr vs. Nb/Th. High Rb/Sr values (indicative of phlogopite in the source region) are correlated with low Nb/Th values. This relationship is consistent with progressive melting of phlogopite from a phlogopite + amphibole lithospheric source, and also with the presence of oxide mineral phases that retain Nb during melting. Both scenarios are consistent with the proposed origin of the CLM source region; see text for discussion.

and suggest that metasomatism of the oceanic lithosphere by small volume silicate melts plays an important role in ocean island magmatism. In the African western rift, model ages for the different isotope systems suggest metasomatic events beneath Nyiragongo at ~490 Ma near the close of the Pan-African (Vollmer and Norry, 1983; Vollmer et al., 1985), and between ~750 and 1000 Ma during the Kibaran orogeny (Rogers et al., 1992; Graham et al., in preparation) for the CLM source. The correspondence of model ages with known orogenic events is consistent with a lithospheric mantle source for the trace and minor element inventory of most western rift volcanics (Rogers et al., 1992). Relics of much older events, perhaps dating to Archean, may also be preserved in their Pb isotope compositions (Rogers et al., 1992; Graham et al., in preparation), but modeling of those multi-stage histories is more uncertain. The pattern of REE/HFSE enrichment observed at Rungwe, Nyiragongo, Toro Ankole and the Tshibinda sector of Kivu (Fig. 7) is indicative of carbonatite metasomatism, but the effects appear to be geographically restricted and may be unrelated to formation of the amphibole- and phlogopite-bearing CLM source. It is worth noting that lavas from two of the areas affected by carbonatite metasomatism, Rungwe and Toro Ankole, have Sr–Nd isotope compositions that trend from the CLM source towards the EACL.

### 3.7. Inferred variations in lithosphere thickness and erosion

Our observations suggest that the CLM source is available beneath the entire African Rift system, an area of roughly 1,000,000 km$^2$. The evidence for amphibole, phlogopite, spinel and garnet in this mantle source suggests that the most prevalent depth of lithospheric melting is roughly 65–80 km. Ultrapotassic lavas from eastern Virunga and Toro Ankole require melting at depths greater than ~80 km, whereas alkali basalts from Rungwe, Huri Hills and Naivasha indicate melting at depths shallower than ~65 km. In addition, other lithospheric mantle sources identified by the range of isotopes and trace elements for individual volcanic areas suggest variations in lithospheric thickness over short distances.

At Huri Hills, and in the Tshibinda and Bukavu sectors of the Kivu province, lavas show trends towards isotope compositions resembling those for some ocean island basalts (HIMU-like, in the terminology of Zindler and Hart, 1986). This observation suggests that there may be a significant sub-lithospheric contribution in these two areas, and that the lithospheric mantle may contribute little, if any, melt to local magmatism. This Kivu mantle source clearly has all the trace element and isotopic (Sr, Nd, Pb and He) characteristics found at HIMU oceanic islands such as St. Helena (Weaver, 1991; Graham et al., 1992, 1995). Based on geochemical arguments alone, the origin of the Kivu lavas is equivocal. They may represent magmas derived by melting of metasomatized subcontinental lithosphere (e.g., McKenzie and O'Nions, 1995). Alternatively, they may have a deeper, mantle plume origin. The presence of a plume in the region is consistent with the geophysical arguments for the uplift of the East African Plateau (e.g., Griffiths and Campbell, 1991). The wide range in isotope and trace element compositions in the Kivu volcanic province, from HIMU type to CLM source values, appears consistent with strong interaction of upwelling plume material with the lithosphere beneath this area. This implies active lithospheric erosion, but confined to a relatively small area in the western rift.

Our inferred lithospheric thickness variations based on geochemical arguments are generally consistent with evidence from gravity surveys and seismic profiles carried out throughout the rift system (e.g., KRISP Working Group, 1987, 1991; Simiyu and Keller, 1997). In the eastern rift, the lithosphere is thinnest beneath the Huri Hills region: seismic profiles and gravity models indicate a crustal thickness of ~20 km and in some areas do not require the presence of any lithospheric mantle (e.g., Hendrie et al., 1994; Simiyu and Keller, 1997). The mantle velocity structure inferred from seismic refraction and wide-angle reflection experiments (e.g., KRISP Working Group, 1987, 1991) suggest that the onset of melting occurs at a depth of ~65 km. This conclusion is compatible with the range of erupted mafic lavas, which include both plume-like (HIMU) compositions and lithospheric melts, as well as the inferred presence of garnet in the mantle source (Class et al., 1994). Both crust and lithosphere thicken away from Huri Hills: garnet- and spinel-lherzolite xenoliths suggest crustal and lithospheric thicknesses of 30 and 45 km, respectively, east of the rift at Marsabit (Henjes-Kunst and Altherr, 1992). Xenolith equilibration temperatures and pressures suggest that the crust thickens to a maximum depth of 42 km and a lithosphere which is ~73 km thick in southern Kenya; the lithospheric thickness increases to ~100 km in northern Tanzania (Henjes-Kunst and Altherr, 1992; Dawson, 1994). Lavas from Naivasha that sample the CLM source therefore occur in an area with crustal thickness between 30 and 42 km, and lithospheric thickness between 45 and 73 km, i.e., at depths of 75–115 km.

In the western rift, our interpretations generally agree with those based on geophysical investigations, although they differ slightly in detail. Geochemical considerations would indicate that the lithosphere is thickest beneath Toro Ankole and the eastern Virunga province. Away from there, the lithosphere thins rapidly westward towards Kivu and gradually southward towards Rungwe. Simiyu and Keller (1997) infer a mantle gravity anomaly at a depth of ~60 km beneath the western rift axis, centered between the Virunga and Toro Ankole provinces. In their model, the depth to the mantle anomaly decreases to 50 km at 3°S latitude (south of the Kivu province), and increases rapidly to the north, where the anomaly cannot be recognized at 3°N latitude. This implies that any actively upwelling asthenosphere is most likely to be present beneath the northern portions of Lake Tanganyika and beneath the southern (Bukavu) sector of the Kivu province. We suggest that elsewhere along the western rift, the asthenosphere has not been able to ascend to sufficiently shallow depths for melting, because tectonic extension and lithospheric erosion are both very limited. This is supported by the observation that many of the lavas erupted in Quaternary time carry a record of melting of a phlogopite-bearing clinopyroxenite source. Our preferred explanation, based on the geochemical and geophysical observations, is that lithospheric erosion (i.e., to depths shallower than ~60–80 km) appears to be restricted in the western rift to the southern portions of the Kivu volcanic province and the northern portions of Lake Tanganyika.

## 4. Summary

Mafic lavas from the Kivu volcanic province display a wide range in incompatible trace element abundances (e.g., crossing REE patterns) and Sr–Nd isotope ratios. All Kivu lavas have elevated incompatible trace element contents relative to MORB and the estimated primitive mantle, requiring that the source region has been enriched by one or more metasomatic events. Samples from Tshibinda volcano, which lies on a major rift border fault at the northwestern margin of the province, have geochemical features that are distinct from the majority of Kivu (Bukavu) lavas. Tshibinda lavas have, for example, the highest values of $^{87}Sr/^{86}Sr$, $(La/Sm)_n$, Ba/Nb, and Zr/Hf observed among Kivu samples. Sr–Nd isotopic values at Tshibinda trend towards enriched compositions found in the neighboring Virunga province, while Bukavu group lavas include the lowest $^{87}Sr/^{86}Sr$ and highest $\varepsilon_{Nd}$ measured in western rift lavas.

The Tshibinda lavas are geochemically distinct within the Kivu province, but their Sr–Nd isotopic compositions and certain incompatible trace element ratios (e.g., La/Nb, Ba/Nb, Rb/Sr) trend towards values that are common to several rift volcanic provinces. Graham et al. (1995) demonstrated that selected lavas from the Kivu, Virunga, Toro Ankole and Rungwe volcanic provinces have Sr–Nd–Pb isotopic compositions that converge upon a narrow range of values, and inferred the existence of a CLM source region. There are consistent trace element characteristics of the CLM source as well, and they help to constrain its mineralogy. This source material appears to be present beneath both the eastern and western rift branches.

The CLM source contains small amounts of both amphibole and phlogopite, as indicated by the geochemistry of mafic lavas and supported by the mineralogy of mantle xenoliths found in northern Tanzania (Dawson and Smith, 1988, 1992). This modal mineralogy requires at least one metasomatic enrichment event, which Dawson and Smith (1988) attribute to ultra-alkaline katungite. Models of REE abundances in mafic rift lavas (Latin et al., 1993; Furman, 1995) and lherzolite xenoliths from Kenya suggest that melting dominantly occurs near the spinel–garnet transition (~60–80 km), where both phlogopite and amphibole are likely to be stable in the continental lithosphere. Based on experimental studies (e.g., Lloyd et al., 1991), some ultrapotassic lavas from Toro Ankole and the Virunga province are derived by melting of a more phlogopite-rich source, and therefore probably originate from somewhat greater depths than the CLM source (cf. Olafsson and Eggler, 1983).

The geochemical evidence allows estimates of variations in lithospheric thickness along the eastern and western rift branches, and these variations are generally consistent with those inferred from geophysical evidence. In the eastern rift, it is significant that the CLM signature is not observed in mafic lavas from Huri Hills, Kenya, where geophysical studies (e.g., Hendrie et al., 1994; Simiyu and Keller, 1997) do not require any lithospheric mantle to be present between the crust and upwelling asthenosphere. Both the crust and lithosphere thicken southward, and in the Naivasha region, their combined thickness may be as much as 75–115 km (Henjes-Kunst and Altherr, 1992; Simiyu and Keller, 1997). In the western rift, the lithosphere is thickest beneath eastern Virunga and Toro Ankole, and thinnest near the Bukavu sector of the Kivu province. These observations suggest that the Kivu province is above a region of active lithospheric erosion, where interaction between upwelling asthenosphere and metasomatized lithosphere produces the very wide range in isotopic and trace elemental signatures of the erupted lavas.

## Acknowledgements

Funding for this research comes from the Earth Sciences Division of NSF (grants 9508112 to T.F., 9304156 and 9614508 to D.G.). We are grateful to C. Ebinger for providing samples, to M. Rhodes and M. Chapman for patient assistance in obtaining XRF analyses, and to F. Frey and P. Ila for their generosity in providing INAA. D.G. thanks George Tilton for graciously providing access to the clean lab and mass spectrometer at UCSB. T.F. thanks A. Upchurch for her careful work in helping prepare the maps. Thoughtful comments from W. McDonough, N. Rogers and an anonymous reviewer helped improve the final manuscript.

## Appendix A. Petrographic descriptions of Kivu thin sections

| Sample | Petrographic description | Percentage of phenocrysts |
|---|---|---|
| R3L | Porphyritic, with 1–2 mm phenocrysts of cpx (zoned) and oliv (3:1) in ground mass of opaque oxides + plag + cpx | 25 |
| R3K | Porphyritic, with 1–3 mm phenocrysts of plag (zoned, twinned, occasionally corroded), oliv (typically corroded), cpx (zoned, twinned, typically corroded, with reaction coronae) (6:3:2) in a groundmass of plag + oliv + opaque oxides | 40 |
| R4HA | Porphyritic, with 1–2 mm phenocrysts of oliv (euhedral), with less abundant plag + cpx (5:2:3) in a groundmass of plag (oriented flow) + cpx + oliv + opaque oxides | 40 |
| R2J | Microcrystalline, with sparse phenocrysts (0.5 mm) of cpx + oliv with rare plag (2:2:1), in a groundmass of plag + opaque oxides | 20 |
| B10C | Microcrystalline, with sparse phenocrysts (1–2 mm) primarily oliv > plag (4:1); oliv replaced locally by serpetine; groundmass of plag + oliv + cpx + opaque oxides | 15 |
| R4Q | Porphyritic, with 0–1.5 mm euhedral phenocrysts of oliv (some rimmed by cpx) + cpx (3:7), replaced locally by serpetine; groundmass of opaque oxides + plag + cpx | 35 |

| | | |
|---|---|---|
| R5A1 | Moderately porphyritic, with phenocrysts (0.5–1.5 mm) of euhedral oliv + cpx (2:3), oliv replaced locally by serpetine and corroded; in a groundmass of plag + cpx + opaque oxides | 40 |
| R5N | Phenocrysts (< 1 mm, euhedral) of oliv + cpx + plag (2:2:1) in a groundmass of plag + oliv + cpx + opaque oxides | 25 |
| R6C | Moderately porphyritic, with phenocrysts of oliv (2 mm) + cpx(1 mm) + plag (0.5 mm) (2:7:1) in groundmass of plag + cpx + opaque oxides | 30 |
| Z7Z | Phenocrysts of plag (∼ 1 mm) + oliv (1–1.5 mm) and minor cpx (1 mm) (2:2:1) in medium-grained groundmass (∼ 0.5 mm) of plag + cpx + opaque oxides | 30 |
| Z3D | Phenocrysts of plag (∼ 1 mm) + oliv (1–1.5 mm) and minor cpx (1 mm) (2:2:1) in medium-grained groundmass (∼ 0.5 mm) of plag + cpx + opaque oxides | 20 |
| Z5G | Sparsely phyric, with 1–2 mm phenocrysts of cpx > oliv > plag (4:3:2) in groundmass of opaque oxides + plag + cpx | 45 |
| Z6A | Porphyritic, with 2–3 mm euhedral phenocrysts of cpx < oliv (2:3), in a groundmass of plag + cpx + opaque oxides | 25 |
| Z6B | Porphyritic, with 2–3 mm euhedral phenocrysts of cpx > oliv (3:2), in a groundmass of plag + cpx + opaque oxides | 30 |

## References


Adam, J.D., Green, T.H., Sie, S.H., 1993. Proton microprobe determined partitioning of Rb, Sr, Ba, Y, Zr, Nb and Ta between experimentally produced amphiboles and silicate melts with variable F content. Chem. Geol. 109, 29–49.

Auchapt, A., Dupuy, C., Dostal, J., Kanika, M., 1987. Geochemistry and petrogenesis of rift-related volcanic rocks from South Kivu (Zaire). J. Volcanol. Geotherm. Res. 31, 33–46.

Baker, B.H., Williams, L.A.J., Miller, J.A., Fitch, F.J., 1971. Sequence and geochronology of the Kenya Rift volcanics. Tectonophysics 11, 191–215.

Baker, B.H., Goles, G.G., Leeman, W.P., Linstrom, M.M., 1977. Geochemistry and petrogenesis of a basalt–benmoreite–trachyte suite from the southern part of the Gregory Rift, Kenya. Contrib. Mineral. Petrol. 64, 303–332.

Bell, K., Blenkinsop, J., 1987. Nd and Sr isotopic compositions of East African carbonatites: implications for mantle heterogeneity. Geology 15, 99–102.

Bell, K., Doyle, R.J., 1971. K–Rb relationships in some continental alkaline rocks associated with the East African Rift valley system. Geochim. Cosmochim. Acta 35, 903–915.

Bell, K., Powell, J.L., 1969. Strontium isotopic studies of alkalic rocks: the potassium-rich lavas of Birunga and Toro-Ankole regions, east and central equatorial Africa. J. Petrol. 10, 536–572.

Bell, K., Simonetti, A., 1996. Carbonatite magmatism and plume activity: implications from the Nd, Pb and Sr isotope systematics of Oldoinyo Lengai. J. Petrol. 37, 1321–1339.

Bellon, H., Pouclet, A., 1980. Datations K–Ar de quelques laves du Rift-ouest de l'Afrique Centrale: implications sur l'évolution magmatique et structurale. Geologische Rundschau 69, 49–62.

Boynton, W.V., 1983. Cosmochemistry of the rare earth elements: meteorite studies. In: Henderson, P. (Ed.), Rare Earth Element Geochemistry. Elsevier, New York, pp. 63–114.

Class, C., Goldstein, S.L., 1997. Plume–lithosphere interactions in the ocean basins: constraints from the source mineralogy. Earth Planet. Sci. Lett. 150, 245–260.

Class, C., Altherr, R., Volker, F., Eberz, G., McCulloch, M.T., 1994. Geochemistry of Pliocene to Quaternary alkali basalts from the Huri Hills, northern Kenya. Chem. Geol. 113, 1–22.

Cohen, R.S., O'Nions, R.K., Dawson, J.B., 1984. Isotope geochemistry of xenoliths from East Africa: implications for development of mantle reservoirs and their interaction. Earth Planet. Sci. Lett. 68, 209–220.

Davies, G.R., Lloyd, F.E., 1989. Pb–Sr–Nd isotope and trace element data bearing on the origin of the potassic subcontinental lithosphere beneath south-west Uganda, Kimberlites and Related Rocks. Geol. Soc. Aust. Spec. Publ., Vol. 14. Blackwell, Perth, pp. 784–794.

Davies, G.R., Macdonald, R., 1987. Crustal influences in the petrogenesis of the Naivasha basalt–comendite complex: combined trace element and Sr–Nd–Pb isotope constraints. J. Petrol. 28, 1009–1031.

Dawson, J.B., 1994. Quaternary kimberlitic volcanism on the Tanzanian craton. Contrib. Mineral. Petrol. 116, 473–485.

Dawson, J.B., Smith, J.V., 1988. Metasomatised and veined upper-mantle xenoliths from Pello Hill, Tanzania: evidence for anomalously light mantle beneath the Tanzanian sector of the East African Rift valley. Contrib. Mineral. Petrol. 100, 510–527.

Dawson, J.B., Smith, J.V., 1992. Olivine–mica pyroxenite xenoliths from northern Tanzania: metasomatic products of upper-mantle peridotite. J. Volcanol. Geotherm. Res. 50, 131–142.

De Mulder, M., Hertogen, J., Deutsch, S., André, L., 1986. The role of crustal contamination in the potassic suite of the Karisimbi volcano (Virunga African Rift Valley). Chem. Geol. 57, 117–136.

Dupuy, C., Liotard, J.M., Dostal, J., 1992. Zr/Hf fractionation in intraplate basaltic rocks: carbonate metasomatism in the mantle source. Geochim. Cosmochim. Acta 56, 2417–2424.

Ebinger, C.J., 1989a. Geometric and kinematic development of border faults and accommodation zones, Kivu–Rusizi Rift, Africa. Tectonics 8, 117–133.

Ebinger, C.J., 1989b. Tectonic development of the western branch of the East African Rift system. Geol. Soc. Am. Bull. 101, 885–903.

Ebinger, C.J., Bechtel, T.D., Forsyth, D.W., Bowin, C.O., 1989. Effective elastic plate thickness beneath the East African and Afar Plateaus and dynamic compensation of the uplifts. J. Geophys. Res. 94, 2883–2901.

Furman, T., 1995. Melting of metasomatized subcontinental lithosphere: undersaturated mafic lavas from Rungwe, Tanzania. Contrib. Mineral. Petrol. 122, 97–115.

Furman, T., Graham, D., 1994. Chemical and isotopic variations in volcanic rocks from the Rungwe Province: constraints on the development and scales of source heterogeneity beneath the African Western Rift. Mineral. Mag. 58A, 297–298, V.M. Goldschmidt Conference.

Graham, D.W., Humphris, S.E., Jenkins, W.J., Kurz, M.D., 1992. Helium isotope geochemistry of some volcanic rocks from Saint Helena. Earth Planet. Sci. Lett. 110, 121–131.

Graham, D.W., Furman, T.H., Ebinger, C.J., Rogers, N.W., Lupton, J.E., 1995. Helium, lead, strontium and neodymium isotope variations in mafic volcanic rocks from the western branch of the East African Rift system. EOS 76, F686.

Graham, D.W., Furman, T.H., Ebinger, C.J., Rogers, N.W., Lupton, J.E., in preparation. Isotope variations in mafic volcanic rocks from the western branch of the East African Rift system: probes of the subcontinental lithospheric mantle.

Griffiths, R.W., Campbell, I.H., 1991. Interaction of mantle plume heads with the Earth's surface and onset of small-scale convection. J. Geophys. Res. 96, 18295–18310.

Harkin, D.A., 1960. The Rungwe volcanics at the northern end of Lake Nyasa. Geol. Survey Tanganyika Mem. II.

Harry, D.L., Leeman, W.P., 1995. Partial melting of melt-metasomatized subcontinental mantle and the magma source potential of the lower lithosphere. J. Geophys. Res. 100, 10255–10269.

Hawkesworth, C.J., Kempton, P.D., Rogers, N.W., Ellam, R.M., van Calsteren, P.W., 1990. Continental mantle lithosphere, and shallow level enrichment processes in the Earth's mantle. Earth Planet. Sci. Lett. 96, 256–268.

Hendrie, D.B., Kusznir, N.J., Morley, C.K., Ebinger, C.J., 1994. Cenozoic extension in northern Kenya: a quantitative model of rift basin development in the Turkana region. Tectonophysics 236, 409–438.

Henjes-Kunst, F., Altherr, R., 1992. Metamorphic petrology of xenoliths from Kenya and northern Tanzania and implications for geotherms and lithospheric structures. J. Petrol. 33, 1125–1156.

Hoernle, K., 1990. The major element, trace element and Sr–Nd–Pb isotopic evolution of Gran Canaria (Canary Islands) magma sources over the past 15 Myr: inferences on the geochemical and structural evolution of the mantle. PhD dissertation, UCSB, 140 pp.

Holmes, A., 1940. Basaltic lavas of South Kivu, Belgian Congo. Geol. Mag. 77, 89–101.

Holmes, A., 1950. Petrogenesis of katungite and its associates. Am. Mineral. 35, 772–792.

Holmes, A., Harwood, H.F., 1937. The petrology of the volcanic area of Bufumbira. Mem. Geol. Surv. Uganda 3, 1–300, Part II.

Ionov, D.A., Griffin, W.L., O'Reilly, S.Y., 1997. Volatile-bearing minerals and lithophile trace elements in the upper mantle. Chem. Geol. 141, 153–184.

Ionov, D.A., Grégoire, M., Prikhod'ko, V.S., 1999. Feldspar–Ti-oxide metasomatism in off-cratonic continental and oceanic upper mantle. Earth Planet. Sci. Lett. 165, 37–44.

Kalt, A., Hegner, E., Satir, M., 1997. Nd, Sr and Pb isotopic evidence for diverse lithospheric mantle sources of East African Rift carbonatites. Tectonophysics 278, 31–45.

Kampunzu, A.B., Mohr, P., 1991. Magmatic evolution and petrogenesis in the East African Rift system. In: Kampunzu, A.B., Lubala, R.T. (Eds.), Magmatism in Extensional Structural Settings: the Phanerozoic African Plate. Springer, Berlin, pp. 85–136.

Kampunzu, A.B., Caron, J.-P., Lubala, R.T., 1986. The East African Rift, magma genesis and athenolithospheric dynamics. Episodes 9, 211–216.

KRISP Working Group, 1987. Structure of the Kenya rift from seismic refraction. Nature 325, 239–242.

KRISP Working Group, 1991. Large-scale variation in lithospheric structure along and across the Kenya rift. Nature 354, 223–227.

Latin, D., Norry, M.J., Tarzey, R.J.E., 1993. Magmatism in the Gregory Rift, East Africa: evidence for melt generation by a plume. J. Petrol. 34, 1007–1027.

LaTourette, T., Hervig, R.L., Holloway, J.R., 1995. Trace element partitioning between amphibole, phlogopite, and basanite melt. Earth Planet. Sci. Lett. 135, 13–30.

Lloyd, F.E., Bailey, D.K., 1975. Light element metasomatism of the continental mantle: the evidence and the consequences. Phys. Chem. Earth 9, 389–416.

Lloyd, F.E., Huntingdon, A.T., Davies, G.R., Nixon, P.H., 1991. Phanerozoic volcanism of southwest Uganda: a case for regional K and LILE enrichment of the lithosphere beneath a domed and rifted continental plate. In: Kampunzu, A.B., Lubala, R.T. (Eds.), Magmatism in Extensional Structural Settings: the Phanerozoic African Plate. Springer, Berlin, pp. 23–72.

Marcelot, G., Dupuy, C., Dostal, J., Rancon, J.P., Pouclet, A., 1989. Geochemistry of mafic volcanic rocks from the Lake Kivu (Zaire and Rwanda) section of the western branch of the African Rift. J. Volcanol. Geotherm. Res. 39, 73–88.

McDonough, W.F., 1990. Constraints on the composition of the continental lithospheric mantle. Earth Planet. Sci. Lett. 101, 1–18.

McKenzie, D., O'Nions, R.K., 1995. The source regions of ocean island basalts. J. Petrol. 36, 133–159.

Menzies, M.A., Murthy, V.R., 1980. Enriched mantle: Nd and Sr isotopes in diopsides from kimberlite nodules. Nature 283, 634–636.

Mitchell, R.H., Bell, K., 1976. Rare earth element geochemistry of potassic lavas from the Birunga and Toro-Ankole regions of Uganda, Africa. Contrib. Mineral. Petrol. 58, 293.

Nelson, D.R., Chivas, A.R., Chappell, B.W., McCulloch, M.T., 1988. Geochemical and isotopic systematics in carbonatites and implications for the evolution of ocean–island sources. Geochim. Cosmochim. Acta 52, 1–17.

Norry, M.J., Truckle, P.H., Lippard, S.J., Hawkesworth, C.J., Weaver, S.D., Marriner, G.F., 1980. Isotopic and trace element evidence from lavas, bearing on mantle heterogeneity beneath Kenya. Philos. Trans. R. Soc. London, Ser. A 297, 259–271.

Olafsson, M., Eggler, D.H., 1983. Phase relations of amphibole, amphibole-carbonate and phlogopite-carbonate peridotite: petrologic constraints on the asthenosphere. Earth Planet. Sci. Lett. 64, 305–315.

Paslick, C., Halliday, A., James, D., Dawson, J.B., 1995. Enrichment of the continental lithosphere by OIB melts: isotopic evidence from the volcanic province of northern Tanzania. Earth Planet. Sci. Lett. 130, 109–126.

Pasteels, P., Villeneuve, M., De Paepe, P., Klerkx, J., 1989. Timing of the volcanism of the southern Kivu province: implications for the evolution of the western branch of the East African Rift system. Earth Planet. Sci. Lett. 94, 353–363.

Rogers, N.W., De Mulder, M., Hawkesworth, C.J., 1992. An enriched mantle source for potassic basanites: evidence from Karisimbi volcano, Virunga volcanic province, Rwanda. Contrib. Mineral. Petrol. 111, 543–556.

Rogers, N.W., James, D., Kelley, S.P., DeMulder, M., 1998. The generation of potassic lavas from the eastern Virunga province, Rwanda. J. Petrol. (in press).

Rudnick, R.L., McDonough, W.F., Chappell, B.W., 1993. Carbonatite metasomatism in the northern Tanzanian mantle: petrographic and geochemical characteristics. Earth Planet. Sci. Lett. 114, 463–475.

Sato, K., Katsura, T., Ito, E., 1997. Phase relations of natural phlogopite with and without enstatite up to 8 GPa: implications for mantle metasomatism. Earth Planet. Sci. Lett. 146, 511–526.

Simiyu, S.M., Keller, G.R., 1997. An integrated analysis of lithospheric structure across the East African plateau based on gravity anomalies and recent seismic studies. Tectonophysics 278, 291–313.

Sun, S.-S., McDonough, W.F., 1989. Chemical and isotopic systematics of oceanic basalts: implications for mantle composition and processes. In: Saunders, A.D., Norry, M.J. (Eds.), Magmatism in the Ocean Basins. Geol. Soc. Lond., pp. 313–345.

Upcott, N.M., Mukasa, R.K., Ebinger, C.J., Karner, G.D., 1996. Along-axis segmentation and isostasy in the Western rift, East Africa. J. Geophys. Res. 101, 3247–3268.

Vollmer, R., Norry, M.J., 1983. Unusual isotopic variations in Nyiragongo nephelinites. Nature 301, 141–143.

Vollmer, R., Nixon, P.H., Condliffe, E., 1985. Petrology and geochemistry of a U and Th enriched nephelinite from Mt. Nyiragongo, Zaire: its bearing on ancient mantle metasomatism. Bull. Geol. Soc. Finland 57, 37–46.

Wallace, M.E., Green, D.H., 1988. An experimental determination of primary carbonatite composition. Nature 335, 343–345.

Weaver, B.L., 1991. The origin of ocean island basalt endmember compositions: trace element and isotopic constraints. Earth Planet. Sci. Lett. 104, 381–397.

White, R.S., McKenzie, D., 1989. Magmatism at rift zones: the generation of volcanic continental margins and flood basalts. J. Geophys. Res. 94, 7685–7729.

Williams, L.A.J., 1972. The Kenya Rift volcanics: a note on volumes and chemical composition. Tectonophysics 15, 83–96.

Williams, R.W., Gill, J.B., 1992. Th isotope and U-series disequilibria in some alkali basalts. Geophys. Res. Lett. 19 (2), 139–142.

Zindler, A., Hart, S.R., 1986. Chemical geodynamics. Ann. Rev. Earth Planet. Sci. 14, 493–571.